# UNIVERSITY OF TWENTE

**Faculty of Electrical Engineering,**
**Mathematics & Computer Science**

# Utilizing ITU Models for Spectrum Monitoring.

## Suggested improvement for P-1546

Miriam Araj
M.Sc. Thesis
April 2025

**Supervisors**

DR. IR. A.B.J. KOKKELER
DR.IR. P.T. DE BOER
DR. Z. MAHFOUZ
IR. W. BAKKER (RDI)

Radio Systems Group
Faculty of Electrical Engineering,
Mathematics and Computer Science
University of Twente
P.O. Box 217
7500 AE Enschede
The Netherlands

# Contents

# Preface and Acknowledge

This work was prepared for the degree of master's in Electrical Engineering \ Radio Systems from the University of Twente, The Netherlands.

This study was conducted under the supervision of the Dutch Authority of digital infrastructure (RDI) to investigate the signal propagation models of the International Telecommunication Union (ITU) and utilize them in the process of spectrum monitoring.

First, I would like to express my deepest gratitude to my supervisors, Dr. Zaher Mahfouz (UT) and ir. Wouter Bakker (RDI). Your support has been invaluable through this journey and your belief in my abilities has pushed me beyond my limits. I'm also thankful for Prof.dr.ir. Andre Kokkeler who provided me with supervision through my entire master studies.

To my parents, thank you for your unconditional love and encouragement. My dad, my first engineer, who made me discover and love the world of engineering. and my mom who always believed in me.

To my husband, Joseph, who surrounded me with love and supported me with patience and understanding. Thank you for standing by my side through every challenge and triumph. I'm lucky to have you in my life.

To all my friends, thank you for your constant encouragement. Your presence was a source of joy and comfort in the hard days. Grateful for the laughter and support you have provided along the way.

To all these incredible individuals, thank you for being a part of this journey and for helping me achieve this milestone.

# List of acronyms

Sorted alphabetically in ascending order.

| | |
|---|---|
| DVB-T2 | Digital Video Broadcasting – Second Generation Terrestrial. |
| e.r.p | Effective radiated power. |
| ITU | International Telecommunication Union |
| LoRaWAN | Long Range Wide Area Network. |
| LOS | Line of Sight |
| MAPE | Mean Absolute Percentage Error. |
| masl | meters above sea level |
| MISO | Multiple-Input Single-Output |
| OFDM | Orthogonal Frequency Division Multiplexing |
| pdf | Probability Density Function |
| RDI | Rijksinspectie Digitale Infrastructuur.<br>“Dutch Authority for Digital Infrastructure” |
| Rx | Receiver. |
| TCA | Terrain Clearance Angle |
| Tx | Transmitter. |

# Abstract

In order to test the accuracy of ITU signal propagation (prediction) models and use them further in spectrum monitoring, this research compares the prediction results of three ITU signal propagation models (P-1546, P-1812, P-2001) with the measurements of field strengths across the Netherlands to define the most accurate model based on the prediction error. Results of the prediction error are then analyzed to investigate potential improvements of the prediction models.

The statistical comparison showed that P-1812 performs better than the other two models. The Mean Absolute Percentage Error (MAPE) of the prediction is equal to 15.1%, which is the lowest among tested models. As P-1546 had the weakest performance with MAPE equal to 25%, a correction is proposed based on an analytical study of the total transmission loss. The proposed correction helped reducing the prediction error by 8 percentage points and improved the model's performance to match the best-fit model.

This thesis is structured into five chapters: starting by an introduction about spectrum monitoring and channel modeling, and the motivation behind this research in Chapter 1. Chapter 2 presents a literature review about the studied propagation models with an overview of the strength and weakness points of each model. Chapter 3 describes the testing setup, and how measured and predicted values were used to evaluate the models' performance. In Chapter 4, the results are presented and analyzed, and an improvement is proposed and tested. Chapter 5 concludes this research and discusses possible future work.

# Chapter 1: Introduction

Wireless communication has evolved remarkably over the years and has become gradually essential where its importance is marked by several milestones. Starting back in the 1800th with the invention of the Telegraph, which can be seen as the earliest form of wireless communication and a revolution in the world of long-distance communication followed by the development of the Radio in the 19th century. The early-20th century witnessed the invention of mobile phones followed by a massive evolution from one generation to another pursued by the official introduction of WIFI in the early 2000s. More recently, the rise of the internet and advancements in satellite technology have further pushed the boundaries, allowing for instant global connectivity.

In all wireless communication forms the goal is similar, that is to deliver a correct and useful message between the transmitter and the receiver. This can only be achieved by understanding the propagation path of this signal and predicting potential interference of disturbing factors that might face the transmitted signal which is known as channel modeling. It is the process of representing the effect of the communication channel on the propagating signal.

Another factor in achieving a useful communication link is ensuring sufficient usage of the available spectrum. This begins with authorization and continues with the correct usage of the license, known as spectrum monitoring.

The combination of channel modeling and spectrum monitoring facilitates more efficient and reliable wireless communication. This efficiency is achieved by getting the theoretical foundation from modeling and real-time data, and practical insights from spectrum monitoring.

This research will study the latest ITU propagation models and try to find the best-fit model according to real-time data of the regular measurements performed by RDI and suggest a correction to improve prediction accuracy.

## 1.1. Background

For any wireless communication, an electromagnetic (EM) wave has to travel through space and reach the receiver to close the communication circuit. According to the rules of physics, this wave will be subject to transmission loss. This transmission loss is a combination of different types of losses including physical phenomena like reflection, diffraction, scattering, absorption, polarization coupling, building entry, and beam spreading loss [1].

Reflection occurs when an EM wave encounters a smooth surface with dimensions very large in comparison with the signal wavelength. Reflected waves that hold a part of the original signal power might interfere constructively or destructively at the receiver. Diffraction occurs when the Line-of-Sight (LOS) between the transmitter (Tx) and the receiver (Rx) is obstructed with a mass comparable in size with the wavelength. According to Huygens' principle [2], an imaginary wave source is formed behind the obstacle causing the signal to travel further and be received at the Rx. Scattering occurs when a wave encounters an obstacle with dimensions on the order of the wavelength or less causing the wave energy to be scattered in different directions. Other factors contribute to the quality of the received signal, such as the operating frequency, obstacles along the path, propagation environment (sea, land), weather conditions like rain or snow, and the relative motion of the receiver.

To build a reliable and high-speed communication system, a channel model is required to consider all the spatial and temporal characteristics mentioned before to meet the performance requirements of the system. Prediction models are tailored to the type of system; therefore, different types of models are present for wireless signal propagation. Some models are concerned with propagation loss, others are concerned with temporal and spatial impairments, and the type of any model can be stochastic, deterministic, or empirical depending on how it was built.

The International Telecommunication Union (ITU) has published throughout the years different models depending on whether the system is (point-to-point) terrestrial [3], Trans-Horizon [4], Satellite [5] , or Earth-Space communication [6]. Point-to-area models like ITU-R P-1546 [7], ITU-R P-1812 [8], and P-2001 [9] are used for planning services that need to cover a wide areas like broadcasting, mobile networks, or safety communications.

Next to a robust channel model, the spectrum needs to be organized and monitored in a way that ensures maximum efficiency and minimum interference to all radio-wave communications, which is known as spectrum management [10]. The ultimate goal of spectrum management is to provide an efficient nationwide and world-wide radiocommunication service. To ensure the spectrum is managed correctly, a variety of tools are needed:

1. Sufficient knowledge of all radio communication facilities formed into a dataset containing all antennas/stations specifications. This is organized via licensing and billing.
2. Spectrum planning scheme for efficient allocation of services.
3. Spectrum monitoring which as they call it in [10] *"serves as the eyes and ears of the spectrum management process"*.

These tools, in combination with further data analysis and periodic inspections, help using the available spectrum in an efficient manner that provides maximum reliability and quality of service.

In general, channel modeling and spectrum monitoring are complementary processes that enhance each other as follows:

On one hand, channel models can predict possible issues in different scenarios. These predictions can be used as input for spectrum management to help set up more effective strategies. On the other hand, spectrum monitoring can provide real-time data on how the spectrum is utilized in different propagation conditions. This data can be used to refine the models and improve their accuracy.

From this perspective, the Dutch Authority for Digital Infrastructure (RDI) wanted to further improve spectrum monitoring by using the latest ITU signal propagation models to automate the process of detecting anomalous signals, which is the topic of the thesis.

## 1.2. Research Problem

The RDI has already started the first step of spectrum monitoring via a nationwide measurement network that consists of 15 measuring antennas. These antennas are spread around the country to continuously measure the electromagnetic field levels as a function of frequency. Every minute, the measuring antenna sweeps over the frequency range [20 MHz – 3 GHz] with a given frequency step and registers the measured field strength in $dB\mu V/m$ . This measured data is used on a regular basis for different types of analysis. However, the data can be used more efficiently by comparing it to equivalent field levels predicted via ITU signal propagation models according to the licensing database. By analyzing the results of this comparison, abnormal behavior of signals can be detected which can later be developed into automatic detection of anomalous signals and serves the goal of spectrum monitoring.

The research goal might seem straight forward. However, these ITU models cannot be guaranteed to give accurate results, which might lead to unreliable conclusions, and these models cannot be directly used in the spectrum monitoring process. Therefore, the ITU models need to be first validated using the available dataset and measurements provided by the RDI and then improved if needed to be suitable for implementing in spectrum monitoring, which is the topic of this thesis.

## 1.3. Research Questions and Objectives

The main goal of this research can be addressed in the following question:

“How can propagation-loss models provided by the ITU be best utilized to automate the process of spectrum monitoring performed by the RDI?”

This question can be broken down into multiple sub-questions justified by the corresponding objectives:

1. What are the key differences between the studied ITU models? What are the potential challenges and limitations in using each propagation model?

   Analyzing the ITU models and identifying key parameters will give an overview of how comprehensive each model is and how sufficient the RDI dataset is to provide all basic parameters for the models.

2. Which model best fits the measured data, and under which circumstances does it become less accurate?

   The error resulted from comparing prediction results with actual measurements draws a primal sentiment towards the closest fit model. Further analysis of the different ways of calculation per model, extra considerations/correction per model, and whether the environment of the Netherlands resembles one of the models more than the others helps clarifying the reasons behind choosing the leading model.

3. What possible solutions are there to improve the prediction accuracy and minimize the error?

   This improvement does not exclusively mean improving the propagation model by implementing corrections to it, but can also be achieved by improving the input parameters of the models which means developing the data currently available for the RDI.

These questions were designed to guide the research process and ensure a comprehensive outcome.

# Chapter 2: ITU Models for Signal Propagation

In the world of rapid evolution of wireless communication systems in the VHF and UHF bands, there is a continuous need for decent signal propagation models to ensure maximum performance of the system and optimum utilization of the radio spectrum.

As mentioned before, ITU has recommendations for both point-to-point and point-to-area links. In this research, our focus will be on point-to-area propagation models for services such as analog/digital radio/TV broadcast, and mobile networks.

Three main models will be studied:

1. P-1546: A point-to-area prediction method for terrestrial services [7].
2. P-1812: A path-specific point to area prediction method for terrestrial services [8].
3. P-2001: A general purpose wide-range terrestrial propagation model [9].

In the following sections, a detailed description of each model will be presented with the strengths and weaknesses of each method.

## 2.1. Propagation Model P-1546

ITU recommendation P-1546 is a method for radio propagation predictions in the frequency range 30–4000MHz and for the path length between 1–1000km [7]. The computer-based implementation of the recommendation takes essential parameters like terminals height, frequency, and path length as an input, and provides the predicted field and the equivalent transmission loss as an output. An extra log-file can be generated with all used/calculated parameters that can be used for further analysis.

P-1546 is an empirical model based on interpolation/extrapolation of the $q$th percentile of the field strength as a function of frequency, path length, and environment. The model provides graphs similar to Figure 1 for multiple frequencies, path type, and percentage of time. Field strength for the exact curve parameters can be read directly from the curves, while all other combination of parameters can be derived from the computer-based implementation of this recommendation, which is fully provided by ITU via [11].

The software implementation of this method depends on a set of 21 parameters where nine of which are mandatory, while the rest are optional to improve prediction quality. Mandatory parameters include the basic requirements for field prediction, such as Tx/Rx height, representative clutter height around the receiver, a flag to show availability of path info, and the Tx effective height. Some of these mandatory parameters can be seen present in Figure 1 like frequency, path zone “land, (warm/cold)-sea”, percentage of time, and path length. The optional parameters are only useful when you have information about the terrain of the studied propagation path. In this case, a path profile can be constructed, which represents the geographical personality of the propagation path in terms of terrain height and ground cover. The path profile can be used to define the optional parameters leading to improved accuracy of the prediction.

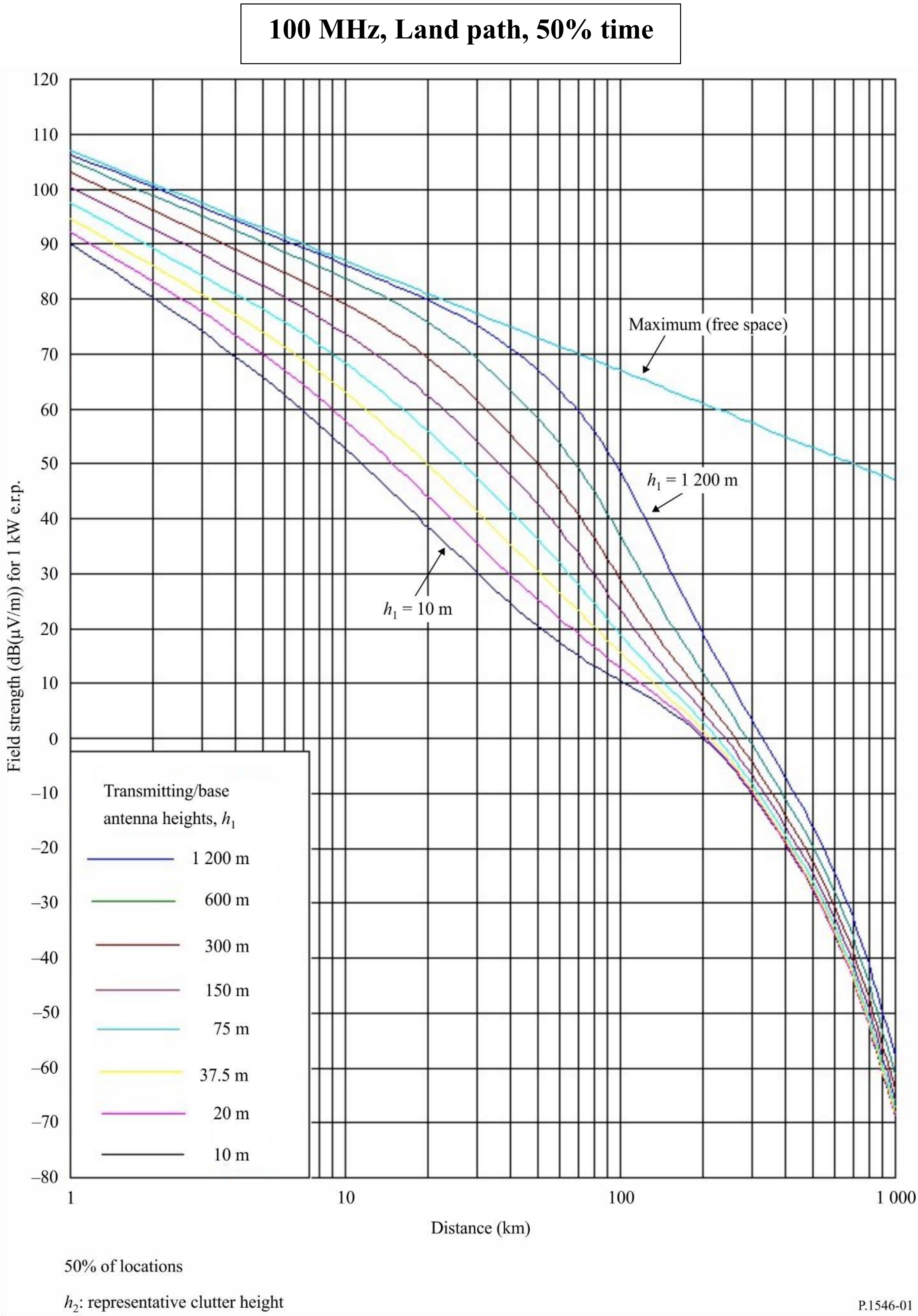


*Figure 1 - Prediction curves for a land path at 100MHz according to propagation model P-1546 [7].*

## Overview of P-1546

### *Transmitting/base antenna height*

As seen in Figure 1, $h_1$, which represents the height of the transmitter in $m$, plays a major role in prediction. Therefore, the model defines it accurately according to different situations. The effective antenna height, $h_{eff}$, is also a major parameter used in most of the cases, defined as the height of antenna in meters over the average level of ground between 3–15 km in the direction of the receiver.

$h_1$is determined as follows:

1. Sea path: $h_1$ is the height of the antenna above the water surface.
2. Land path shorter than 15 km:
    a. *No terrain information available*: $h_1$ is equal to the actual antenna height above ground for paths shorter than 3 km or related to the path length $d$ $[km]$ and, $h_{eff}$,when $3\ km < d < 15\ km$.
    b. *Terrain information available*: $\mathrm{h}_1$ is related to antenna height above ground between 0.2d and d.
3. Land path longer than 15 km: $h_1 = h_{eff}$.

### *Corrections*

To enhance the accuracy of the predictions, the model applies multiple corrections to account for various factors related to the available information of the propagation path. Total predicted field as a result is given by

$$E_{tot} = E_{1kw} + corrections \tag{1}$$

$E_{1kw}$: predicted field strength for 1 kw e.r.p $[dB\mu V/m]$

Three major corrections are applicable:

- Terrain clearance angle correction

  This correction takes the obstacles close to the receiver into account. Mainly, it depends on the terrain clearance angle (TCA) which is the "*elevation angle of the line from the receiving antenna that clears all obstacles in the direction of the transmitting antenna over a distance up to 16 km, but not beyond the base antenna*" [7].

- Receiving/mobile antenna height correction

  This correction accounts for the elevation angle of the received signal depending on the ground cover surrounding the receiver. The value of this correction in [dB] is determined according to a parameter representing the height at which the receiver would experience a grazing incident, called representative clutter height $R_2'$ in (m) proportional to $h_1$ and $d$.

According to the value of, $R'_2$, and the propagation conditions and environment, the correction is determined as elaborated in [7].

- Cluttered transmitter correction

  This correction should be applied in all cases of a cluttered transmitter (even when Tx is higher than the clutter). Its value is frequency dependent and determined whether the clutter at Tx is higher or lower than the antenna itself.

## Literature Review of P-1546

Various research has evaluated the performance of this model in different environments and conditions. An Empirical study in [12] compared measurements performed between the Netherlands and the United Kingdom with prediction results of P-1546, which resulted in random differences up to 20 dB. Another measurement campaign was conducted in Beijing, China, in a high-dense urban environment [13]. The results showed that in most circumstances, the measured transmission loss is larger than the predicted loss by P-1546. In Brazil, the model was tested using a 563 MHz carrier and compared with measurements of the same reference signal from 27 locations in a vegetation environment of an unregular terrain covered by forest [14]. Results of the pathloss mean error and standard deviation came out high in comparison with other models tested in the same research.

Other research was dedicated to improving the accuracy of this prediction model by applying modifications and correction factors. Paran and Noori in [15] proposed an optimization algorithm for tuning the model parameters and reducing prediction error in different propagation environments. Another study in [16] shows the effect of clutter height around the receiver on the prediction accuracy and suggests a correction factor that accounts for the environment and the clutter height around the receiver. Authors in [17] proposed a new definition for the transmitter height. $h_1$.that is suitable for distances less than 15 km. The proposed definition solved the reciprocity problem of the model and improved the prediction quality.

## 2.2. Propagation Model P-1812

ITU recommendation P-1812 is a prediction method for point-to-area terrestrial services in the range 30 – 6000 MHz[8]. It predicts signal levels exceeded for a given percentage of time $p\%$ in an average year and a given percentage of locations $P_l\%$. This method is suitable for path lengths between 0.25 – 3000 km and can handle terminals height up to 3km above ground.

The computer-based implementation of this propagation model requires, as an input, some path-specific parameters related to the actual terrain and clutter heights along the propagation path in addition to the essential parameters related to the terminals' height and the operating frequency. As an output, the electrical field strength in $dB\mu V/m$ and equivalent transmission loss in $dB$ are presented. Log files provide detailed analysis of all types of losses based on the terrain profile. Therefore, it is suitable for planning a service area in terms of desired coverage, and for considering the reduction of this service duo to possible interference.

P-1812 is a deterministic approach based on calculating the basic transmission loss and equivalent field strength. The model takes into account various propagation mechanisms and is highly dependent on the path profile which represents the geographical personality of the propagation path. This requires an accurate source for geographical data to obtain terrain height information, and ground cover information called clutter data, which can be derived from digital maps.

Using the geographical database, the model establishes a path profile that contains information about the effective heights of terminals, the great-circle path distance, and Tx/Rx elevation angles for trans-horizon paths.

To make calculations more accurate, the model splits the path into multiple equal sub-sections where the start/end of each sub-section is marked by a profile point. The number of profile points is proportional to the path length. For each profile point the terrain height, clutter height, and distance to the transmitter should be known where Tx is the 1st profile point and Rx is $n^{th}$.

## Overview of P-1812

### *Transmission Loss*

This model takes into consideration various propagation mechanisms like: LOS propagation, diffraction, tropospheric scattering, and ducting/layer reflection. The combined effect of this mechanism forms a foundation to the total propagation loss which is later corrected by including the effect of building entry attenuation and location variability.

1. Line-Of-Sight propagation

The part of the transmission loss that is related to free space propagation. Generally, it is proportional to operating frequency and the distance between Tx/Rx.

2. Propagation by diffraction

Diffraction loss is calculated by combing two terms from two diffraction estimation methods:

- the Bullington construction: cares for the transition between free-space and obstructed propagation. This first term of the total diffraction loss is also a combination of applying same Bullington construction twice: One using the actual path profile, and the other using a zero-height smooth profile where the terrain is considered completely flat.
- Spherical-Earth diffraction: This is the part of the diffraction loss related to the earth curvature and the terrain electrical properties which differs between land and sea paths.

3. Propagation by tropospheric scattering

When the signal is intended to travel for long distances beyond the horizon, propagation is possible via the lowest layer of the atmosphere “called troposphere”. Due to the nature of this layer, only a small portion of the transmitted power would scatter back to the receiver, therefore, the loss due to tropospheric scattering, $L_{bs}$, needs to be considered. It is however limited by the free space transmission loss, $L_{bfs}$, where $L_{bs} \geq L_{bfs}$ to avoid underestimating it.

4. Ducting/layer reflection

At sufficiently high frequencies and suitable region and climate, the troposphere can form a guide for radio waves propagation with much lower losses than tropospheric scattering; known by duct propagation. When ducting occurs, the signal levels will be intensified as the wave is allowed to travel beyond line of sight. In all cases, the model calculates the loss related to ducting. This loss is compared to LOS loss to identify the type of propagation and calculate the total transmission loss accordingly.

## Additional Considerations

### *Location variability of losses*

When planning mobile networks, it is critical to consider the variation of signal strength according to the environmental clutter and the terrain variation when the receiver is moving. The model suggests, according to broad data analysis, that the mean field strength due to clutter variation is lognormally distributed and its standard deviation. $\sigma_L$. is dependent on the frequency and the width of area where this variability is applied.

### *Building entry losses*

As explained by ITU recommendation P-2040 [26], if one terminal is inside a building or structure, additional loss must be considered. P-1812 considers field strength variation for indoor reception as a function of location variability, $\sigma_L$, and building entry attenuation, $\sigma_{be}$.

## Literature Review of P-1812

To evaluate the performance of this prediction method, multiple studies have tested the model in different environments and compared results to actual measurements and other propagation models. In the study presented in [18], measurements in the FM band collected by a car-mounted setup in different environments in Novosibirsk, Russia were compared with prediction results from P-1812 method and resulted in a low standard deviation compared to P-1546 and Longley-Rice models. In the DVB-T band, the model was tested in a forest environment [14] and in an urban environment [19] and compared with actual measurements, results presented by both papers show that the error standard deviation of P-1812 is lower than other tested models.

Some research also tested the validity of P-1812 when planning for Internet-of-Things technologies like Low Power Wide-Area Networks (LPWAN). The study in [20] showed that P-1812 is indeed a suitable model for Low Range Wide Area Networks (LoRaWAN).

As this model is highly dependent on Terrain and clutter data, a lot of studies show the effect of optimizing the clutter or terrain database as in [21].

In general, this model offers best performance in the majority of studies related to comparing prediction models owing to the detailed path analysis and the ability to fitting in different environments and situations.

## 2.3. Propagation Model P-2001

Different from the previously discussed models, P-2001 is a general-purpose prediction method for terrestrial propagation in the range 30 MHz to 50 GHz [9]. Therefore, it can be used for different point-to-point or area-to-point predictions for land, sea, or mixed paths. The model predicts the transmission loss in $dB$ not exceeded for a given percentage of an average year and proved to be most accurate between 3–1000 km. However, it can be suitable for shorter distances only when terminals are high enough to avoid the domination of the effect of clutter with no limit for maximum terminal height. This method is symmetrical; hence the terms transmitter and receiver are only used for convenient marking of the beginning and end of the propagation path.

Similar to P-1812, this method is a deterministic approach that constructs a path profile and base the calculations according to it. Therefore, terrain data is essential for the prediction process.

### Overview of P-2001

*Transmission Loss*

This method is considered a general-purpose prediction method as it uses 4 sub-models to evaluate the transmission loss. These sub-models are then integrated to accurately represent the statistical relationship among them. The sub-models are defined as follows:

1. Sub-model 1: considers normal propagation close to the ground, involves the effects of diffraction, precipitation fading and non-ducting clear air effects.
2. Sub-model 2: considers propagation due to atmospheric stratification, involves the effects of ducting and layer reflection.
3. Sub-model 3: considers the irregular air motion caused by winds in diverse speeds and directions, known as atmospheric turbulence. It involves the effects of precipitation fading and troposcatter.
4. Sub-model 4: considers the loss of sporadic-E reflection that is using the lower level of the Ionosphere to propagate radio waves.

### Additional Considerations

The sub-models described before are propagation mechanisms that deliver a full link between the transmitter and the receiver. However, there are some aspects that do not provide a full path but form an additional attenuation on the already mentioned four links.

P-2001 model accounts for three additional attenuation sources. These are detailed as follows:

### *Gaseous absorption*

This attenuation occurs due to certain gases when signals travel through the atmosphere, primarily Oxygen and water vapor. The effect of this attenuation depends on multiple factors such as frequency, atmospheric pressure, temperature and the condensation of water vapor. Higher frequencies are more sensitive to this kind of attenuation as the size of these molecules becomes comparable to the wavelength.

ITU has a separate recommendation, P-676-11 [22], discussing attenuation by atmospheric gases. However, P-2001 also accounts for gaseous absorption by calculating the loss due to Oxygen, and water vapor under (non-)rain conditions.

### *Precipitation attenuation*

It is the attenuation caused by the absorption of radio frequency signals by rain, snow, and ice.

The propagation path can be classified as rain or non-rain path according to the climatic zone of both Tx/Rx defined via their longitude and latitude.

The full attenuation prediction is the ITU method P-838-3 [23]. This method takes into account the variation of rainfall throughout an average year and calculates the attenuation coefficient for a given rainfall.

## Literature Review of P-2001

Unlike what has been previously discussed for the other two models, P-2001 is not widely studied for field prediction or validation. This model is used for more case-specific predictions as it considers various kinds of losses. Authors in [24] studied the capabilities of P-2001 to be used for modeling beyond-LOS communication through tropospheric scattering and investigated the effect of measuring conditions and various parameters on the prediction accuracy. Kevicera *et al*. [25] investigated in their paper the Delta-Bullington diffraction model that is implemented in P-2001. They empirically proved that this model provides better results with lower complexity in terms of computational requirements in comparison with other models. Which makes it preferable when considering interference analysis.

## 2.4. Chapter Summary

The chapter discussed the latest point-to-area ITU propagation models “P-1546, P-1812, P-2001” that will be used in this research. These models are designed to deliver the expected transmission loss and the expected field strength at the receiver as an output, when corresponding transmitter parameters are presented as an input. The main potentials of each model were explained, and the special features were highlighted to show capabilities of each model. A small literature review was conducted per model to analyze strengths and weaknesses, point out the models’ performance in different environments and conditions, and get an overview of possible improvements.

# Chapter 3: Methodology and Setup

In this chapter, the test environment is described. The first part explains how the measurements are obtained and prepared to be used for testing. The second part describes how the input parameters of the models are obtained and processed to serve the research. Some additional considerations to improve the results quality are also elaborated in 3.5.

## 3.1. Test Methodology

To evaluate the performance of the three mentioned prediction models, prediction results will be compared with the measurements performed by RDI. These measurements are assembled via a measuring network involving 15 fixed antennas spread all over the country as seen in Figure 2.


*Figure 2 – RDI measurements network.*

## 3.2. General Approach

A test scenario is established to organize the evaluation procedure. At each test run, all transmitters within a specific range around the receiver (later determined as 100 km) are considered as illustrated in Figure 3. The field strength is predicted per Tx/Rx link, and then the cumulative field of all individual links is calculated and compared to the RDI measurements.

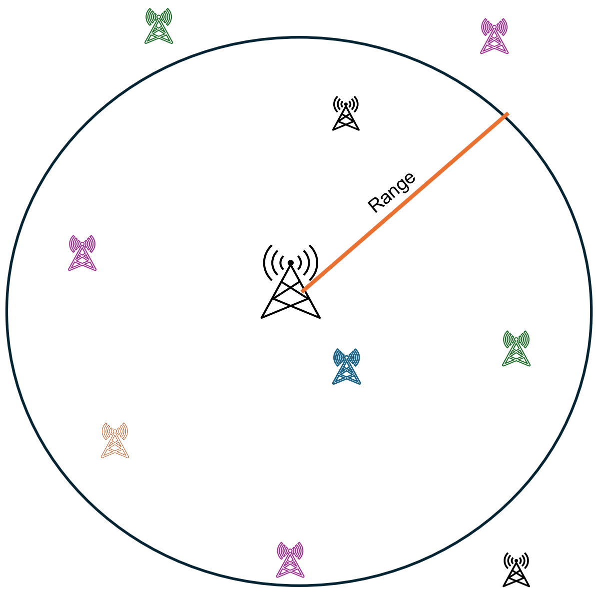

*Figure 3 – An illustration of a test run.*

To know which transmitters are within the specified range, the distance between each Tx in the Netherlands and all 15 measuring locations are calculated using MATLAB and registered as extra information in the RDI transmitters dataset.

The prediction error, which is the measure to compare the performance of the three models, is defined as

$$prediction\ error = prediction - measurement \tag{2}$$

Therefore, a negative error means the measured field is higher than expected.

RDI sets $\mp 5\ dB$ as a threshold for an acceptable error.

Testing is performed in the digital video broadcasting band (DVB-T2), i.e. [470 – 698 MHz]. Twenty four frequencies within this range are operating in the Netherlands. A single test run is a combination of one frequency/location. therefore, within the specified range, all transmitters working on the given frequency in that location are considered in the process of field prediction as illustrated in Figure 3.

## 3.3. Reference Measurements

Each of the 15 fixed measuring antennas performs a sweep over frequencies every minute registering the measured field strength in $dB\mu V/m$. Results are registered in a MATLAB data structure per day. Each structure contains the following information.

a. Longitude/Latitude of the measuring antenna. (it will be referred to as receiving antenna henceforth).
b. Measurements date.
c. Start/Stop frequency of this dataset ($F_{start/stop}$).
d. Frequency step ($F_{step}$).
e. Antenna type and filter bandwidth.
f. Number of data points representing the number of steps available in this frequency range.
g. Number of minutes with measurements. Ideally, it should be equal to $24h \times 60mins = 1440$. However, this number might be less by $2 \sim 3$ regarding the start/stop minutes.
h. Data measurement time.
i. Measurements matrix: containing the actual measured field strength in $dB\mu V/m$ per frequency step per minute, therefore, its size is equal to : $number\ of\ minutes\ with\ measurements\ \times number\ of\ data\ points$.

It is important to clarify that when the measuring receiver is sampling a value, it is always sampling a voltage, $U_r$. The input impedance of the measurement receiver, $Z_i$, is normally 50 Ω. Hence, the received power is given by

$$P_r = \frac{U^2}{Z_i}$$

Using antenna theory, the received electric field strength, $E$, is given by

$$E = \sqrt{\frac{P_r}{A_r} . Z_0}$$

$A_r$ : The effective antenna area $[m^2]$.

$Z_0$: The propagation impedance of free space, equal to 377 Ω.

Combining the previous equations results in the formula

$$E = U_r \sqrt{\frac{1}{A_r} \cdot \frac{Z_0}{Z_i}}$$

The square root in the previous formula is known as the antenna factor, $K_a$. As discussed in the book of C.*Balanis [27]* , the antenna factor is a parameter that relates the field strength received by an antenna to the voltage produced at its output terminal, usually expressed in $dB/m$ or $m^{-1}$. The field strength as a simple expression is then given by:

$$E = U_r . K_a$$

The antenna factor is known for all measurement antennas and is already applied before saving the measurements.

For the predicted value, a small process is applied to retrieve a value suitable for comparison. Our interest is in the difference between the transmitted power and the received field strength. Therefore, we can convert the predicted received power into a voltage assuming a $50\ \Omega$ input impedance and directly compare the result into the value registered in the measurements file.

The predicted received power, $P_r$, is calculated from the predicted transmission loss, $L_b$, which is delivered as an output by each model given that the transmitted power, $P_{t(e.i.r.p)}$, is known:

$$P_r|_{dBW} = P_t|_{dBW} - L_b|_{dB}$$

The received power is converted into a voltage assuming $50\ \Omega$ input impedance as follows:

$$V|_{dB\mu V} = P_r|_{dBW} + 120 + 20\log_{10}\sqrt{Z_i} = P_r|_{dBW} + 137$$

Assuming $K_a = 1$, which is only true in this case as the measuring equipment is correcting for the antenna factor, the received power is then related to the received field strength by:

$$E|_{dB\mu V/m} = P_r|_{dBW} + 137$$

This predicted field strength can be directly compared to the corresponding field strength in the measurements file.

To find the exact needed measured value for comparison, a block from the measurement's matrix mentioned in i. is retrieved. This block is centered around the column with the transmitting frequency, $F$, that has the index $index = F - (F_{start}/F_{step})$. The width of this block is related to the channel bandwidth. e.g. a DVB-T2 channel is 8MHz, therefore, the block to consider is covering the columns

from $index - (4MHz/F_{step})$ to $index + (4MHz/F_{step})$

For digital audio/video broadcasting service in the Netherland, Orthogonal Frequency Division multiplexing (OFDM) is used. In OFDM signals, the transmitted power is evenly distributed across the signal bandwidth as discussed in [28]. At the receiver side, the measurement equipment is a band scan antenna with a filter bandwidth of $6\ KHz$ and a step of $200KHz$. According to the filter specifications, the measurements block retrieved in the previous step will not cover the full $8MHz$ DVB-T channel but only a fraction of it, and the power measured over the entire block does not resembles the power received over the full DVB-T channel. Therefore, the ideal case for comparison is to correct the transmitted power by bandwidth ratio, $bw = \frac{filter\ banwidth}{channel\ bandwidth}$, and calculate the predicted received field strength expected over 6KHz. For the measured field strength, only 1 column of the retrieved measurements block will be considered which contains the measured field strength over 6khz bandwidth over 24 hours. Taking the average over the measuring period will resemble the average measured field strength at the given frequency/location.

Various research has discussed whether the average or the median should be used, as in the study presented in [29]. Research has justified that the median is less sensitive to extreme values and remains unaffected by outliers. In our study, the effect of outliers is definitely present next to other factors that might increase the noise level for small periods. This can affect the measurements and shift the normal distribution of the sample into a skewed distribution. In this case, the average can be pulled into the direction of the skew while the median provides a better measure of the central tendency. Therefore, it is preferred to use the median when dealing with data that possibly contains outliers.

Next to the theoretical reasoning, couple rounds of testing were run to compare the prediction error using median and average measured field strengths. Results show that the prediction error using the median is indeed smaller in most of the cases as seen in Table 1.

*Table 1 – Prediction error using average vs. median values in [dB].*

| Location | Frequency | P-1546 | | P-1812 | | P-2001 | |
|---|---|---|---|---|---|---|---|
| | | average | median | average | median | average | Median |
| **Breda** | 642 | -9.2 | -7.8 | -2.3 | -0.9 | -3.40 | -2.01 |
| **Amstelveen** | 490 | -16.7 | -15.8 | -1.9 | -1.0 | 1.44 | 2.40 |
| **Heerhugowaard** | 578 | -2.2 | -2.0 | 2.8 | 3.0 | 3.03 | 3.23 |

## 3.4. Propagation Models' Setup

In order to run the tests, various parameters are required to implement the software version of the models using MATLAB. Therefore, a MATLAB script was built to extract the required parameters from the available sources, calculate some parameters to improve the accuracy, pass everything to ITU models to get predictions, and finally compare and visualize the results.

### Common parameters

Each model needs some specific parameters depending on the model's type. However, all models need the basic information like operating frequency, height, location, power, etc. These can be derived directly from the RDI database.

The mentioned database is visually present on “Antenna Register” [30]. This public website contains all up-to-date registered transmitters in the Netherlands sorted according to the application (mobile communication, broadcasting, amateurs) or according to generation (2G, 3G, etc.) or mobile networks. Each separate antenna has its own information including operating frequency, height above ground, transmitting power, and the degree of the main lobe in the case of a directional antenna.

The same database can be extracted as an Excel sheet where additional information is provided such as: the exact location of the transmitter as latitude/longitude combination, polarization, and the antenna pattern as 36 values (0°– 360° with a 10° step) of e.r.p reduction in dB for vertically/horizontally polarized component according to the polarization for directional antennas.

## Exclusive parameters

As explained before, P-1546 deals with the propagation path as a united section while models P-1812 and P-2001 need to build a path profile where the total propagation path is split into multiple profile points. The number of profile points is proportional to the total path length.

For all the calculations in these models, 3 main parameters need to be known for each profile point: distance to the transmitter, terrain height, and clutter height.

In this path profile, each profile point is marked by its latitude/longitude which is used to calculate its distance to the transmitter. Same location details can be passed to the digital maps to find the terrain and clutter heights.

Terrain data examine the land's topography showing the elevation above sea level and distinguishing between land and water areas. This type of information can be retrieved from a digital elevation map (DEM). The DEM used for this research was a Geotiff file of the Netherlands in WGS84 format in a resolution of 50 meters, provided by the RDI.

Clutter data include the height of all man-made buildings/structures above the ground, which is essential for diffraction and scattering calculations. Clutter info can also be found via digital maps. The map used in this research is a Geotiff map with a resolution of 400 meters where the country is classified in 49 clutter classes.  Each class was assigned an approximate height to be used as clutter height.

## 3.5. Additional considerations

### Testing range

To make sure the effect of all available transmitters is involved in the predicted field, all transmitters located at 100 km or less from the measuring location are considered.

The 100 km range was determined based on trial and error. The prediction error stabilized around 85 km as seen in Figure 4 indicating that this is a good range to consider.

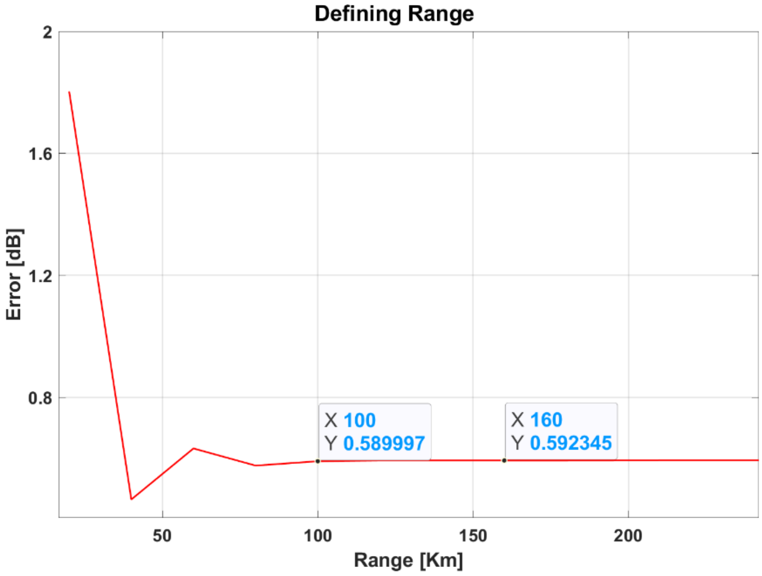


*Figure 4 - Defining "Test Range".*

Theoretically, fields at greater distance than 100 km will have negligible effect on the total predicted field. Therefore, these transmitters can be excluded from the test.

### Phase coherence

As explained in the general approach, signals of individual links are combined at the receiver in order to estimate the total field at a given frequency. This procedure simulates a type of Multiple-Input Single-Output (MISO) system.

One of the essential aspects when combining these signals is phase. The phase of each received signal consists of the initial phase at the transmitter, $\phi_0$, plus the phase difference caused by the distance, $d$, that the wave travels relative to its wavelength, $\lambda$, known by propagation delay or phase delay, $\Delta\phi$.

This research have no accurate information regarding the initial phase of each transmitter. Adding a random initial phase, $\phi_0$, to the phase delay, $\Delta\phi$, will require long Montecarlo simulation which is not doable. Therefore, two scenarios where tested:

a. Scenario (A): Transmitters are assumed synchronized (initial phase is zero). However, amplitudes do not add up coherently but according to the phase delay of each component caused by different pathlengths. This delay is given by

$$\Delta\phi = 2\pi\, d/\,\lambda$$

As a result, the final predicted field is given by

$$\sum_{i=1}^{n} E_i \, e^{j\,\Delta\phi_i}$$

$n$:number of transmitters in the considered range

$E_i$:field strength of the $i^{th}$ transmitter predicted by the model

$\Delta\phi_i$:phase delay of the signal transmitted by the $i^{th}$ transmitter

b. Scenario (B): Transmitters are assumed asynchronous and the total received power is the sum of powers received from individual links. The signals arriving at the receiver could interfere constructively or destructively due to phase difference, therefore, summing up the received powers will account for this uncertainty by considering the total power regardless of phase differences. Furthermore, summing up the received power simplifies the calculation process by eliminating the need for complex phase alignment or long Montecarlo simulations. Consequently, the total predicted field strength, for scenario B, will be the result of adding up the predicted received powers as follows

$$E_{tot} = \sqrt{\sum_{i=1}^{n} |E_i|^2}$$

## 3.6. Chapter Summary

In this chapter, the research methodology and the test structure were explained. the final evaluation measure which is the prediction error consists of two values: the prediction which is obtained from the models and the measurement which is obtained from the RDI measuring network. Section 3.3 explained how to process the measurements and set them in a form suitable for comparison. Section 3.4 discussed how to obtain and process all the input parameters of the models in order to get the predicted field.

The last section clarified the role of phase and distance in the final predicted field and presented multiple possible scenarios, given that the predicted value is a vector sum of a number of individual links.

# Chapter 4: Results and Analysis

This chapter consists of three main parts. First, the results of implementing the tests of Chapter 3 are introduced and explained. Then, the results are further analyzed to find in which scenarios the models performed poorly and to investigate the possibility of improvement. At the end of the chapter, a modification for the propagation model P-1546 is suggested and tested, and a comparison is performed to show potential improvements.

## 4.1. Phase coherence scenarios

As argued in 3.5, the approach for handling the phase of the received signal has an impact on the total predicted field strength. Therefore, two scenarios were tested. Scenario (A) where phase is defined solely by the propagation delay, $\Delta\phi$, and scenario (B) where phase is eliminated, and the predicted field strength is a result of adding up predicted received powers.

Results in **Error! Reference source not found.**, shows the difference between predicted fields according to scenarios A&B for a sample of 25 pairs of predicted field strengths. Results show that the predicted fields might have a difference with a maximum of 9 $dB$ and a mean of 1.5 $dB$. Analyzing the samples with high differences, it has been observed that these cases had higher number of transmitters contributing to the final field, and the propagation path is longer than 20-25 km. These observations can be explained based on the fact that higher number of components adding up non-coherently means higher possibility for constructive/destructive addition of amplitudes of the received signals. Furthermore, despite the exact location of terminals is specified by longitude/latitude, the phase delay cannot be guaranteed accurate as the $d/\lambda$ ratio is in the range of meters and, $\Delta\phi$, cannot be assured accurate unless, $d$, is precisely defined, which is not possible in our case. Therefore, although adding up predicted received powers, as in scenario B, might have higher prediction error in some cases, as to be seen later, it simulates a realistic propagation environment considering each individual link as a component of a multipath propagation in a time-variant model.

As a result, henceforth, Scenario (B) is going to be followed where all transmitters are assumed asynchronous with no information available about the initial phase, and the total predicted field strength is calculated by adding up predicted received powers.

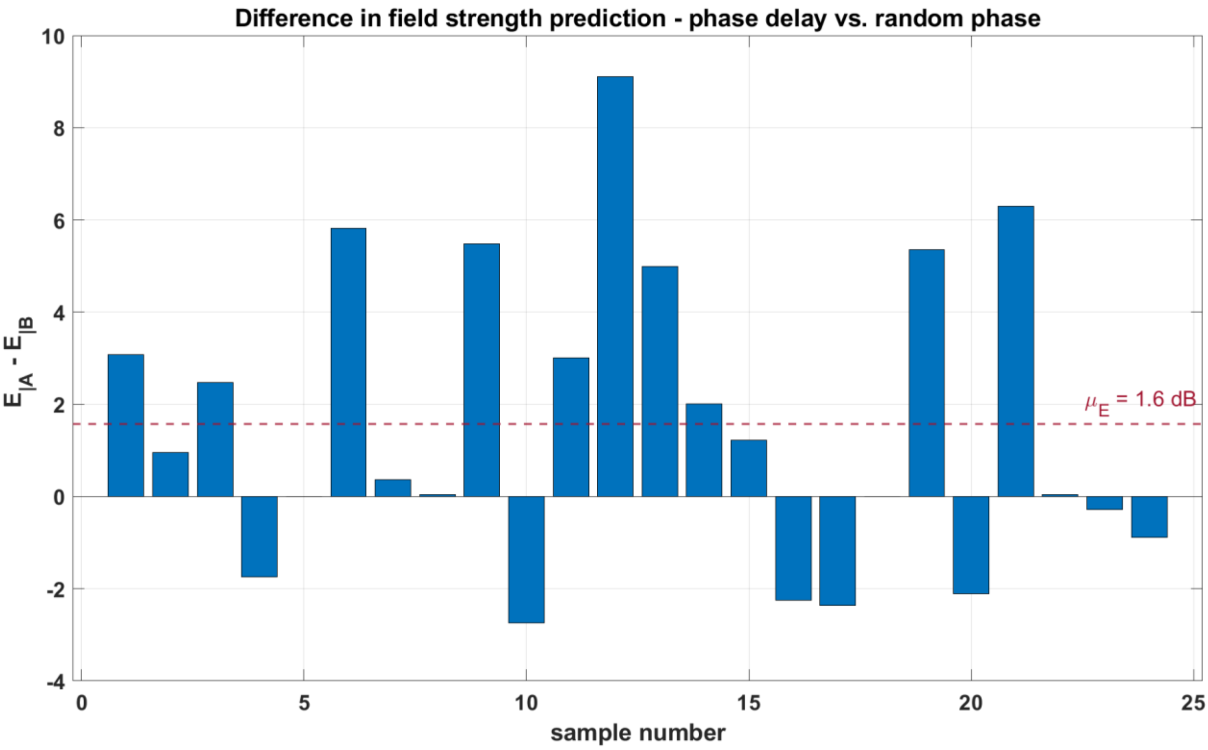


*Figure 5 - Effect of phase coherence. Difference in field strength predicted via scenario A vs. scenario B.*

Before looking into the accuracy of the propagation models and investigating the prediction error, it is important to confirm that these models are modeling the propagation channel realistically, so the predicted values are reliable for comparison.

In an urban environment, similar to where the predictions and measurements were performed, multiple objects can attenuate and scatter the propagated signal, and the probability of non-LOS communication is high. Therefore, no dominant component is expected. On the other hand, the simulated environment is a MISO system as explained in chapter 3, and the received signal is a superimposition of two or more uncorrelated signals approaching the receiver through different propagation paths. According to chapter 5 in the book of *Andreas F Molisch* [28], in such a propagation environment, the system can follow a time-variant multipath propagation model where the envelope of the received signal is expected to be Rayleigh distributed. As all terminals are static, no doppler shift is expected to be present in the received components. However, the received power is expected to be highly variable due to Rayleigh fading.

The histogram showed in Figure 6 resembles the predicted magnitude of the received field strength arriving at one of the 15 fixed receivers at a given frequency for a period of time. Assuming fixed and asynchronous transmitters, received amplitudes are not expected to add up coherently but according to a time-varying phase shift resulting in a Rayleigh distributed envelope of the received signal. Which is indeed the result of Figure 6.

As the power variations are due to Rayleigh fading, the received power, which is the square of the magnitude, is expected to follow an exponential distribution. This is indeed the result seen in Figure 7. When the received power is exponentially distributed, it indicates that the power is highly variable with high probability of experiencing deep fades. This is usually the case in environments with rich scattering and no dominant LOS component, which corresponds to the urban test environment.

Given that the distribution of both amplitude and power of the received field correspond to what is expected by theoretical knowledge, it can be confirmed that the propagation models are simulating the propagation channels in a realistic manner and the results are reliable for comparison with real measurements.

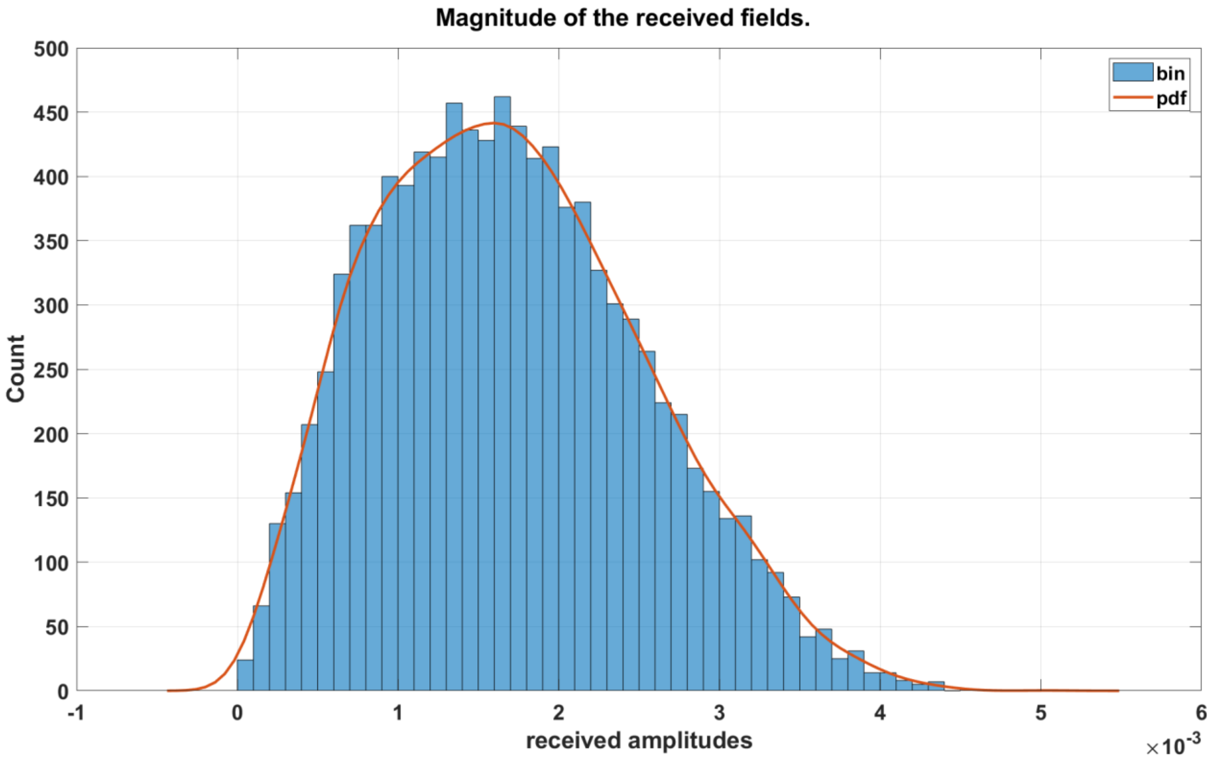


*Figure 6 - Received field strength, static Tx/Rx, asynchronous transmitters.*

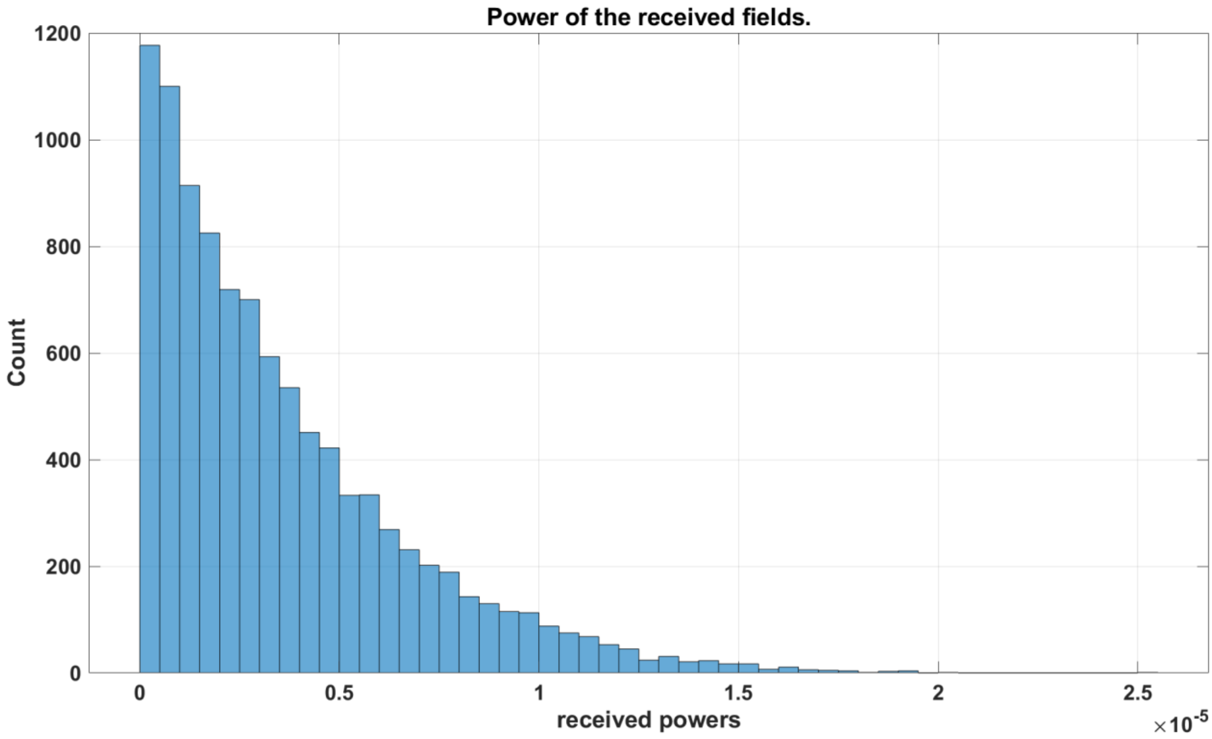


*Figure 7 - Received powers, static Tx/Rx, asynchronous transmitters.*

## 4.2. Prediction error

As explained in the previous chapter, a MATLAB script is built to perform the test elaborated in 3.2, and obtain the prediction error per model defined as:

$$error = prediction - measurement\ [dB].$$

For all the frequencies in the DVB-T2 band, the errors between the field strength predictions and their corresponding measurements are calculated. Next, the median error among the different frequencies is obtained per location per model and is presented in Figure 6.

As Figure 6 indicates, both propagation models P-1812 and P2001 has a median prediction error for the majority of the locations within the acceptable range of $\mp 5dB$. For Some locations, higher prediction error is observed for all models, which indicates possible transmitters' technical issues or license violation in that area. Some measuring locations close to the borders (Germany and Belgium) might experience signal leakage (Interference) from transmitters working on the same frequencies in the neighboring countries, which should also be taken into account. However, this is not considered in this research due to lack of information regarding transmitters in the neighboring countries.

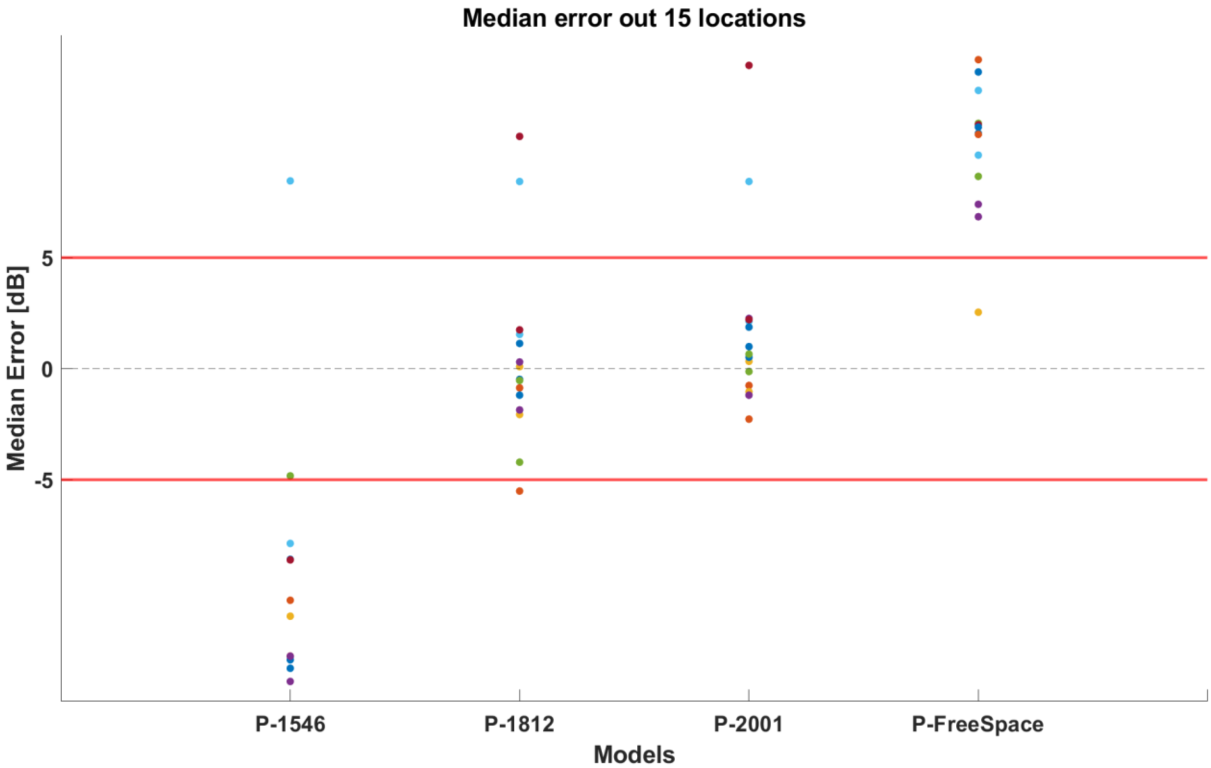


*Figure 6 - Median error of testing in DVB-T2 frequency band.*

Appendix B contains the numerical results of median error per model/location for further elaboration.

Figure 7 presents the probability density function, $pdf$, of prediction errors over all available frequencies/locations. It can be seen that all $pdf_s$ of prediction error are normally distributed which implies that most of the prediction errors are small with larger errors being increasingly rare, indicating that the models are performing well in general. Results of Both P-1812 and P-2001 models are symmetrically distributed around a mean close to zero. This indicates that these models do not have a systematic bias towards overestimating or underestimating the received field strength. The symmetrical distribution also signify that the models' performance is consistent across different data points which means both models are reliable.

Given that both P-1812 and P-2001 models performs very similar, and have low prediction errors, they can both be reliably used for spectrum monitoring. However, as P-1812 has a mean error, $\mu_{P1812} = -0.04\ dB$, which is almost negligible, this model will be considered the best fit model for the rest of this research and will be used for further analysis.

The prediction errors of P-1546 are also normally distributed with a mean around $-11.5\ dB$. The negative mean of the prediction error implies that the measured value is always higher than the predicted value, meaning that the model tends to underestimate the field strength resulting in a high negative error. P-1546 is one of the models currently being used in the Netherlands for the purpose of planning new permits and ensuring availability as well as reliability of the digital infrastructure. Therefore, the research aims to study the reasons why P-1812 outperforms other models and what aspects can be improved in P-1546 in order to improve its accuracy.

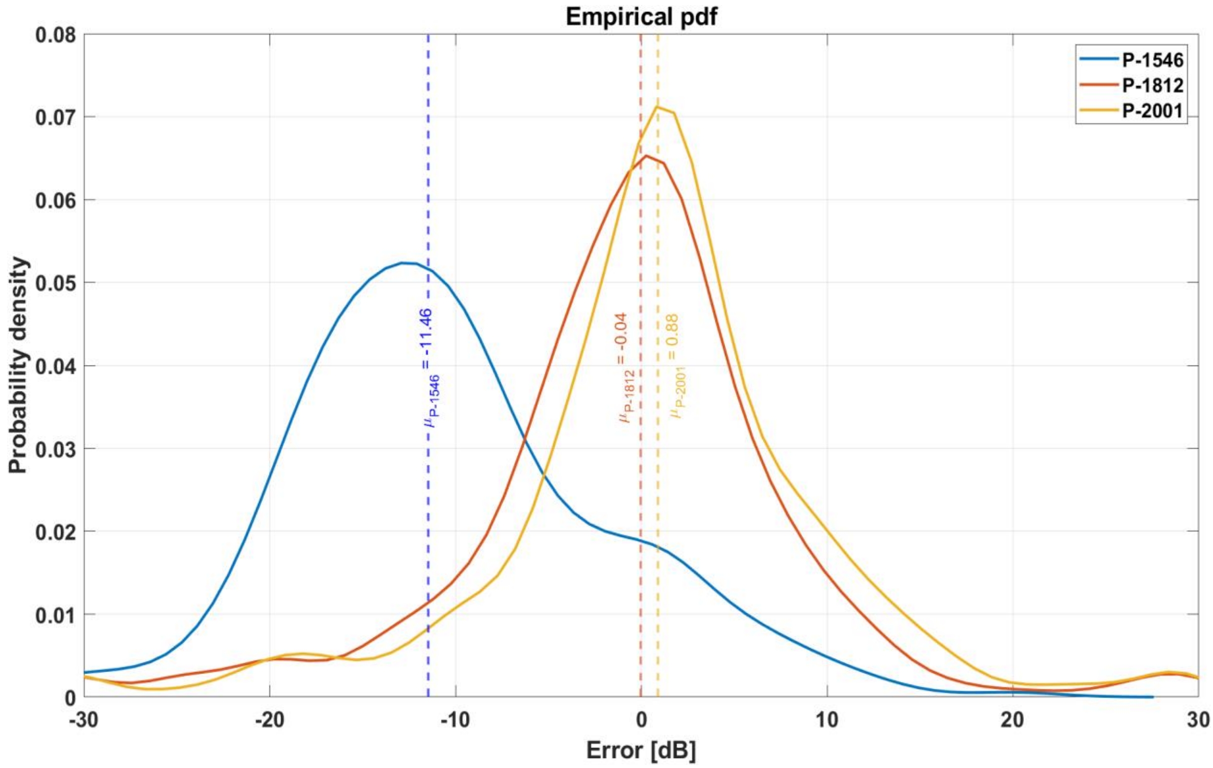


*Figure 7 - Empirical pdf of the prediction error.*

## 4.3. Analysis

By analyzing the log files provided by the models, the following observations can be made:

### Clutter height effect

The digital clutter map used for this research only classifies the clutter into 49 classes according to clutter type but does not actually provide heights in meters. The height assigned to each class has an extensive influence on the results. Therefore, the height for each class was set as the median of the appropriate range in meters for that clutter class, plus a random integer within the same range to ensure comprehensiveness as not all buildings belonging to same clutter class have the exact same height.

### Terrain height effect

Via the log files, it was noticed that models define the effective height, $h_{eff}$, of the terminals differently.

P-1546 defines the Tx effective height as “The height of the antenna above the terrain height averaged between distances of 3 to 15 km in the direction of the receiving station” and the Rx effective height as “either the representative height of ground cover around the receiving/mobile antenna location, or 10 m” [7].

P-1812 uses a smooth-earth model to calculate effective height as elaborated in [8]. This model depends on the variations of terrain heights along the propagation path, known as the path profile, and replaces the actual terrain by a smooth surface with height proportional to the path profile.

In paths where the terrain height varies a lot along the path, the model might be oversimplifying the path leading to underestimating the transmission loss which results in high error.

Although the Netherlands is considered a “flat land” with an average of 3–5 meters above sea level (masl) in most of the landscape, some locations can rise up to 50–60 masl as in ‘t Harde or even over 100 masl in very few areas like Sittard where transmitters/receivers might be available.

Figure 8 gives an example about how (ir)regular the path profile might be. Each sub-figure represents a Tx/Rx path between a transmitter somewhere working on the given frequency and the nearest measuring antenna.

The greatest part of the terrain in the Netherlands is similar to what we see in the example of Breda in Figure 8.a, where the height varies in the range of $\mp 10m$. The example of Figure 8.b shows that the path can have two completely different profiles where a part of it is randomly varying and the other part is flat, and the example of Sittard in Figure 8.c shows the randomness feature of the path profile.

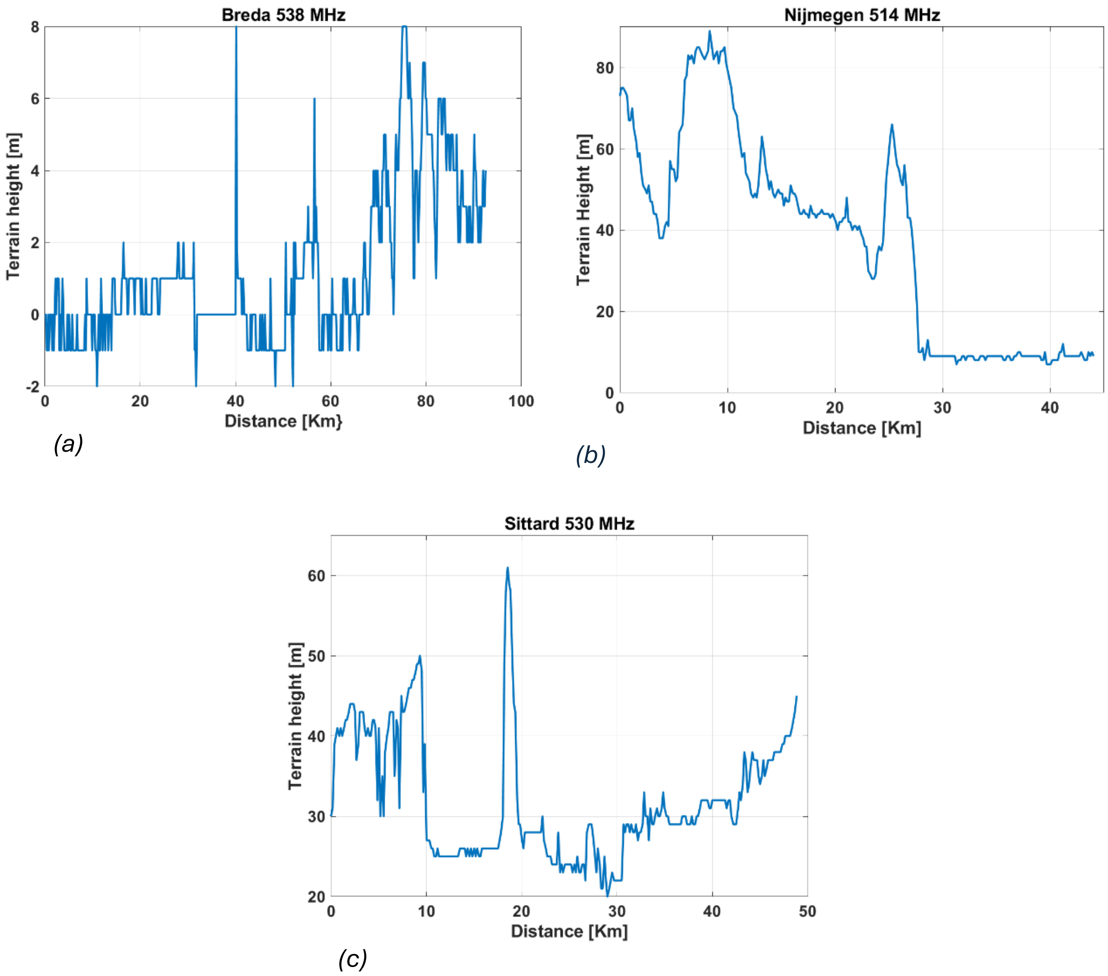


*Figure 8 - Terrain examples.*

As explained in 2.1, the height has a major effect on the prediction result; hence, two trials were conducted to evaluate how heights definition affects the results:

a- Redefine, $h_{eff-Tx}$, in P-1546 as the height of the antenna above terrain height averaged between the distance between Tx/Rx (complete path) and not only between 3-15 km from Tx (begin part of the path)

b- Reduce the effect of smooth-earth model in P-1812 used to calculate, $h_{eff}$, by scaling the smooth-earth height according to the variation of the terrain heights along the propagation path. Results of this modification are presented under the name P-1812-modified. Further elaboration on this modification is presented in Appendix A.

For these trials, three different cases were tested. In each case, we compare the terminal effective height and the prediction error for both models.

1- Nijmegen: similar terminals heights, and similar prediction error. The benchmark for possible corrections.
2- Breda: similar terminals heights, different prediction errors.
3- ‘t Harde: different terminals heights, different prediction errors.

Trial "a" came out with results very similar to the begin case, and the effective height value did not change by redefining it. This shows that the terrain close to the receiver (second part of the path) does not have major effect on the prediction and the definition of, $h_{eff}$, by P-1546 might be left unchanged.

Results of trial "b", where the effective height is inversely related to the terrain variation along the path, came out as presented in Table 2.

As can be observed by the red values in Table 2, reducing the effect of smooth-earth model can influence the effective height confirming that, $h_{eff}$, is directly related to the terrain variations. However, for model P-1812, changing the effective height of terminals does not have a major effect on the prediction error. Therefore, reducing the effect of the smooth-earth model does not improve the prediction accuracy, and the model might be left unchanged.

*Table 2 - Results of trial "b". Heights are in meters and errors in dB.*
*Red colored values are the comparable values changed by the trial.*

| | P-1546 | | | P-1812 | | | P-1812 - modified | | |
|---|---|---|---|---|---|---|---|---|---|
| | $\mathbf{h_{eff-Tx}}$ | $\mathbf{h_{eff-Rx}}$ | **Error** | $\mathbf{h_{eff-Tx}}$ | $\mathbf{h_{eff-Rx}}$ | **Error** | $\mathbf{h_{eff-Tx}}$ | $\mathbf{h_{eff-Rx}}$ | **Error** |
| **Breda** | 116.4 | 42 | -12.6 | 120 | 42.2 | 0.7 | 120 | 42 | 0.7 |
| **Sittard** | 81.9 | 42 | -10.9 | 89 | **50.5** | -0.1 | 89 | **42** | -0.3 |
| **Nijmegen** | 177.7 | 39 | 2.6 | **174.5** | 40.2 | 2.4 | **146** | 39 | 2.4 |

## Definition of transmission loss

As explained in 2.2, the P-1812 method estimates transmission loss deterministically depending on the path profile and compensates for the factors that play a role in the final outcome. This transmission loss is a combination of free space path loss , $L_{fs}$, diffraction loss $L_d$, and troposcattering loss $L_s$.

On the other hand, P-1546 predicts the transmission loss from the equivalent field strength predicted graphically via curves that were built empirically. According to the method's documentation, the predicted field is limited by the free space field strength for 1 kW e.r.p., $E_{fs}$. Therefore, the free space loss, $L_{fs}$, is present. The method is also capable of predicting the field strength for tropospheric scattering, $E_{ts}$, and the equivalent loss, $L_s$, can be derived directly from that. However, the method only considers diffraction when the transmitter's effective height has a negative value, which is the major difference between models P-1546 and P-1812.

Diffraction helps signals to propagate beyond LOS, and its effect is higher in urban environments where lots of obstructions like buildings can be present. By neglecting the effect of diffraction, the total transmission loss might be overestimated as the signal boost caused by diffraction is neglected which leads to lower field predictions, and negative errors in our research, which is exactly the case as seen in Figure 6 and Figure 7.

A proposed modification is to include diffraction loss in the loss prediction of P-1546 without requiring any extra parameters regarding the path profile (e.g. Terrain or clutter map).

## 4.4. Modified P-1546

ITU provides the P-526 recommendation which is propagation by diffraction [31]. This recommendation provides a solution to calculate diffraction loss over isolated obstacles, thin screens, or a finitely conducting wedge when detailed obstacles' information is available. Where no obstacles' information is available, the recommendation provides "Diffraction over a spherical Earth" method to calculate diffraction loss for frequencies at 10 MHz and above at any given distance.

According to this method, diffraction loss is given by

$$20\log\frac{E}{E_0} = F(d) + H(h_1) + H(h_2) \tag{3}$$

Where:

$E$ : Received field strength related to diffraction.

$E_0$: Field strength in free space at same distance.

$d$ : Distance between terminals [km].

$h_1$& $h_2$ : Terminals height above the earth surface[m].

$F(d)$ : Function representing influence of distance [dB].

$H(h)$ : Height-gain [dB].

There are two ways to calculate the distance effect and height gains:

1. Ready to use nomograms provided directly be the model as in Figure 9. Via these nomograms, the functions, $F(d)$, $H(h)$, representing the influence of distance and antenna height respectively can be retrieved by extending the straight line that connects the operating frequency with the corresponding path length or antenna height. Results of these functions can directly be applied in equation 3 to calculate the diffraction field strength, $E$, relative to free-space field strength, $E_0$, at the same distance. Different scales are available according to the effective earth radius factor, $k$, which is an essential parameter used in radio wave propagation to account for the curvature of the earth and the refractive properties of the atmosphere mainly for long-distance communications and radar systems as defined by the ITU in [32]. For standard conditions, $k = 4/3$, which is the ratio of the effective earth radius to actual earth radius.
2. A numerical method which follows the same concept but provides numerical equations that help automating this process. This method is fully elaborated in the documentation of P-526 [31].

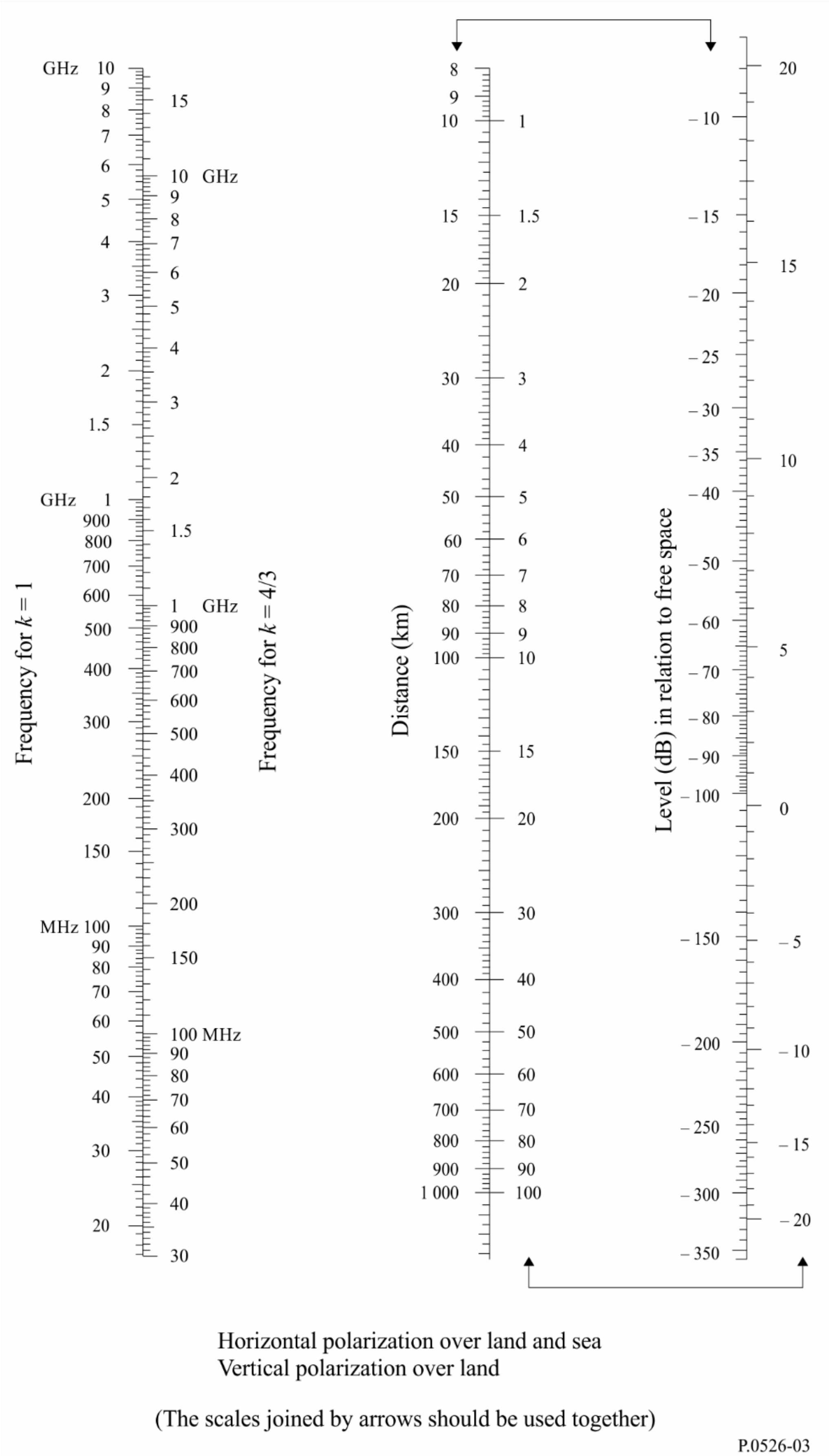


*Figure 9 - Effect of distance on diffraction loss [31].*

The transmission loss of the modified model, P-1546-mod, can be built as follows:

1. Diffraction loss, $L_d$, is calculated via the numerical method of P-526 described in Chapter 4.4.
2. Free space path loss, $L_{fs}$,and troposcattering loss, $L_s$, are already calculated via P-1546 and can be used directly.
3. Losses are combined as described in [8] and the total transmission loss is then given by

$$L_b = -5\log(10^{-0.2L_s} + 10^{-0.2L_{fs+d}})$$

where:

$L_s$: Troposcattering loss [dB].

$L_{fs+d}$: Linear sum of free space loss, $L_{fs}$ ,and diffraction loss, $L_d$. [dB]

The equivalent field strength can be found by

$$E = 139.3 - L_b + 20\log(f_{MHZ})$$

Applying the proposed model and recalculating the prediction error resulted in an improved performance of the P-1546.

In comparison with results In Figure 6, the median error in all tested locations via the modified version of the model P-1546 is decreased to become within the acceptable range as shown in Figure 10, and very close to P-1812 which is the best fit model.

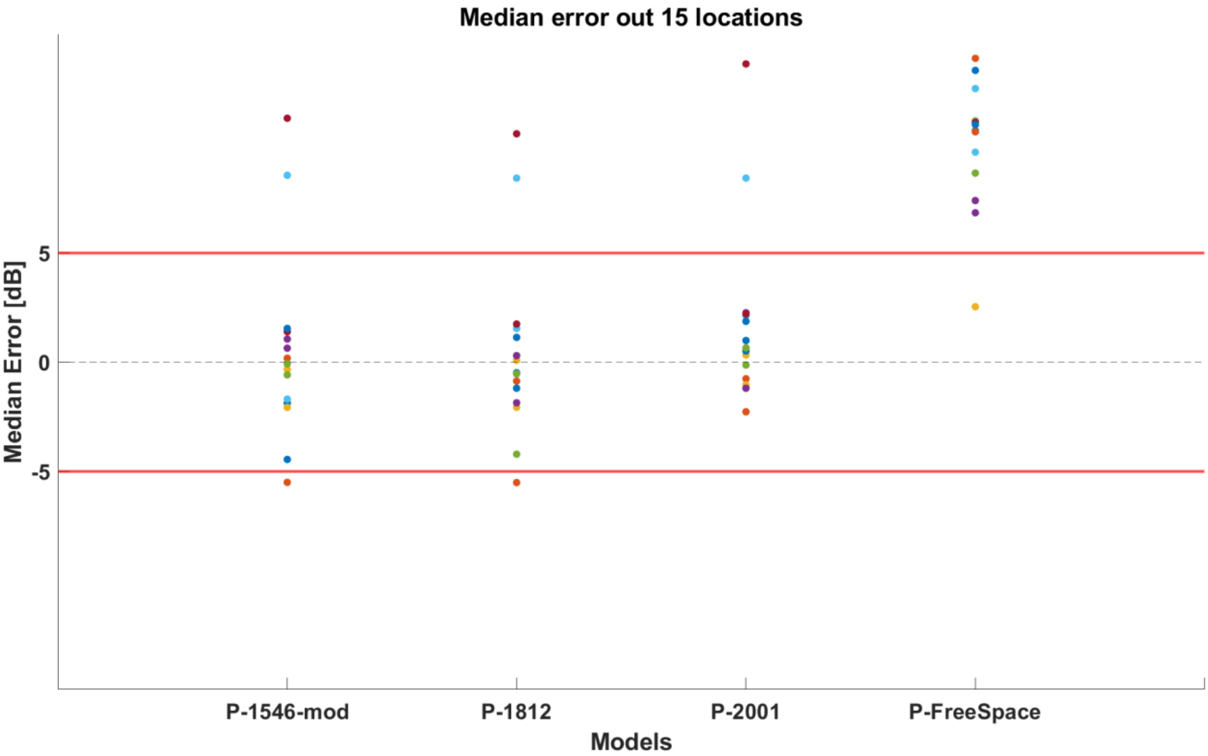


*Figure 10 - Median error of testing in the DVB-T2 frequency band considering the modification of P-1546.*

Figure 11 visualizes the improvement in the modified P-1546 model via the probability density function of the prediction error. As observed in Figure 11, the distribution of the prediction errors is shifted around 11 $dB$ to become centered around a mean value very close to zero and the tendency to underestimate the received field strength is corrected.

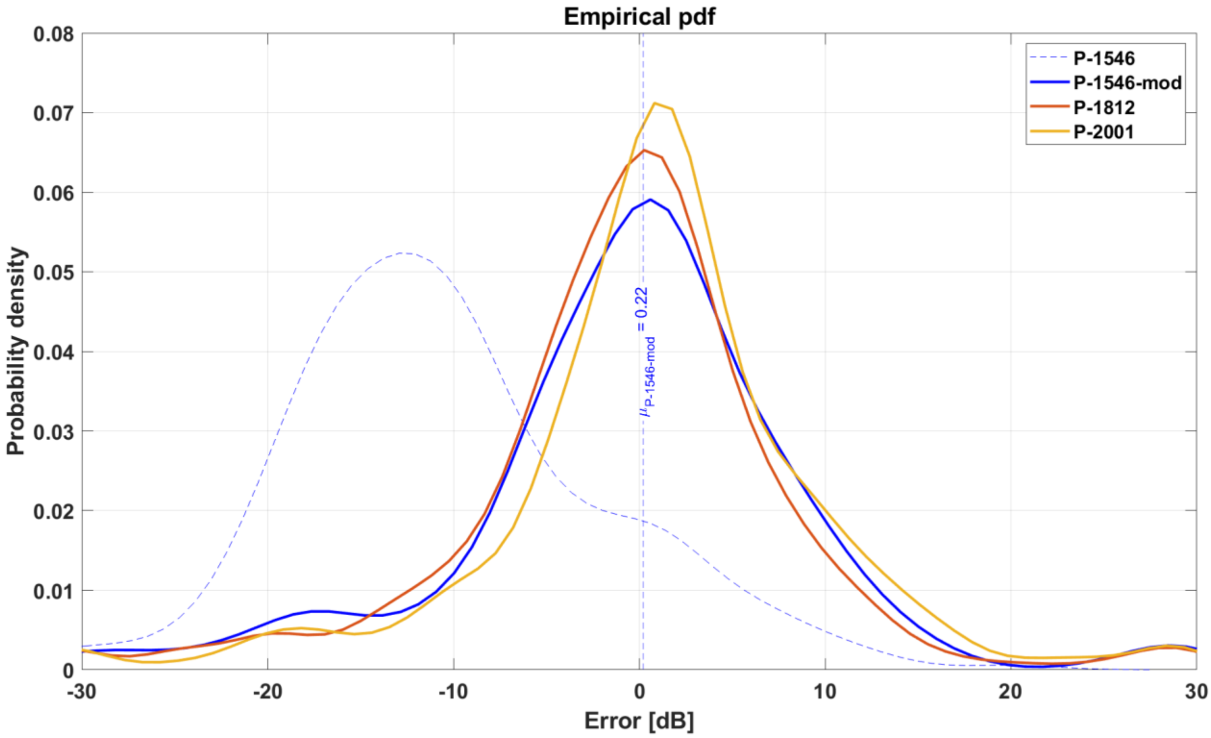


*Figure 11 - Empirical pdf of the prediction error - modified P-1546.*

Results show that incorporating the diffraction model into the P-1546 significantly enhances the prediction accuracy by accounting for the interaction between electromagnetic waves and large obstacles, especially that tests were performed in an urban environment.

Multiple factors with the ability to amplify this loss are relative in this research case:

- Large obstacles with sharp edges and corners are present in buildings in urban environments which can increase diffraction.
- The relatively low frequency of the UHF band used for DVB-T2 which allow waves to propagate for larger distances on one hand and offer more obstacles on long paths on the other hand, leading to higher diffraction.
- Climatic conditions of the Netherlands play a role in increasing diffraction loss; The Netherlands in known to have a cool, cloudy, and humid climate throughout the year with high rainfall; The persistent moisture due to rainfall creates an extra challenge for signal propagation, while frequent cloud cover can further attenuate signal strength.

## 4.5. Mean Absolute Percentage Error (MAPE)

A final matric to evaluate the performance of the propagation models and show the improvement of the modified model is the Mean Absolute Percentage Error (MAPE) which is a measure expressed as a percentage to evaluate the accuracy of prediction methods by calculating the average absolute error between predicted and measured values.

MAPE is given by the formula

$$MAPE = \frac{1}{n}\sum_{i=1}^{n}\left|\frac{A_i - F_i}{A_i}\right| * 100$$

Where:

$n$: the number of observations.

$A_i$: the measured value at observation $i$.

$F_i$: the predicted value at observation $i$.

A table with calculated MAPE for each location is presented in Appendix C.

The Average MAPE over all 15 locations is shown in Table 3.

*Table 3 – Average MAPE of all locations.*

| ***P-1546*** | ***P-1546-mod*** | ***P-1812*** | ***P-2001*** | ***Free Space*** |
|---|---|---|---|---|
| *25.0 %* | *16.8 %* | *15.1 %* | *15.7 %* | *27.9 %* |

Results in Table 3 shows that P-1812 has the lowest MAPE among original models which confirms that it is the best fit model. An improvement of 8.2 percentage points is achieved via the modification of P-1546 which in general makes it give better results and quite close to the best fit model.

As observed before, P-2001 delivers very good results as well, given that it does not require as much parameters as other models which is one of the advantages of this model.

# Chapter 5: Conclusion and Future Work

## 5.1. Conclusion

As a further step to automate the process of spectrum monitoring in the Netherlands, this research was conducted to identify the best-fit signal propagation model and study possible improvements.

The main goal was to answer the three research questions mentioned in Chapter 1.3 regarding the following points:

1. The key differences between the latest ITU models; the potential challenges and limitations in each of them.

A literature study compared the three ITU models "P-1546, P-1812, P-2001" in terms of complexity related to the required parameters, and the level of propagation path knowledge. The review also summarized the studies already done for validating and testing on all three models in different conditions and environments and showed the strength and weakness points of each model.

A point of strength for P-1812 is the ability to calculate different types of loss (diffraction, troposcatter, etc.) when sufficient path information is available. On the other hand, P-1546 can only deliver total transmission loss, no matter what kind of data is available, due to the empirical manner of obtaining predicted fields.

2. Defining the best-fit model

Depending on real measurements of field strength performed by the RDI, A computer-based comparison was performed in the DVB-T2 frequency band between [470 – 698 MHz] using the $prediction\,error\ = prediction\ -\ measurement$ as an evaluation measure.

Results indicated that P-1812 gave highest prediction accuracy with a mean error around$-0.04\ dB$ and a standard deviation of $10.9\ dB$.

P-2001 came in second place with a mean error of 0.9 $dB$ and a standard deviation of $11.2\ dB$.

P-1546 gave the worst results with a mean error of $-11.5\,dB$ indicating an underestimation of the received field strength which enquired further analysis.

3. Possible solutions to improve the prediction accuracy

As the P-1812 and P-2001 prediction models gave quite good results, the choice was to search for possible improvements for the model with lower quality performance, that is P-1546. Another reason to choose this model is the fact that this model is one of the models currently being used in the Netherlands for the purposes of planning and ensuring reliability of the digital infrastructure. Therefore, a modification for the P-1546 was proposed by implementing a correction to account for diffraction loss which resulted in an improvement in the accuracy of this prediction model and reduced the median error by ~8 percentage points making the normal distribution of the error centered around $0.2\ dB$ with a standard deviation of $\sim 12\ dB$.

The research also examined the effect of the phase coherence in simulating realistic propagation environments. Furthermore, the research conveys the role of parameters quality, like terrain and clutter information, in improving the prediction accuracy, particularly for path-specific models. As an example, the original clutter maps were only able to classify clutter into classes. By assigning a suitable height value to each class and adding a random variable within the same height range, the models where able to use the clutter map more comprehensively while preserving the particularity of each class.

## 5.2. Future work

Each of the studied propagation models is able of delivering the predicted transmission loss and the predicted received field strength as an output. In this research, the approach of using the predicted transmission loss was used to arrive to the received field strength (Approach I) as illustrated in Figure 12. After the research was concluded, it has been noticed that using the other approach where the delivered field strength predicted by the models is directly used for the comparison with the measured field strength (Approach II) might be simpler, but the results were slightly different.

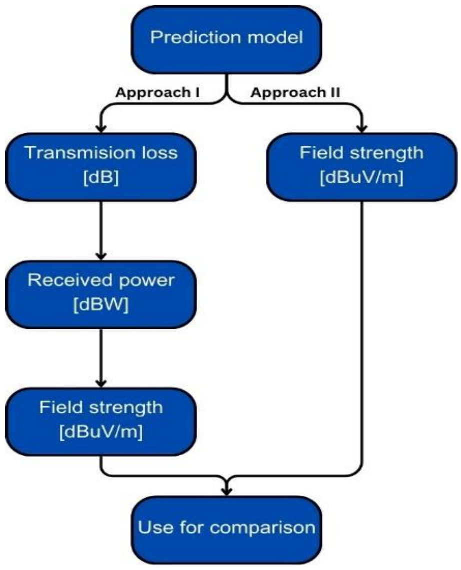


*Figure 12 - Different approaches to arrive to predicted received field strength.*

As to be observed in Figure 13 the probability density functions of the prediction error is similar in distribution in both approaches, but the curves using Approach II are actually shifted towards the left by $\sim 5 - 6\ dB$. Multiple arguments might play a role in this difference, however, this research will not search the details of this difference, and this investigation can be left as a future work for the RDI to consider. Worth noting that the modification suggested for the model P-1546 is still valid as it helped reducing the prediction error by $\sim 10dB$. This aligns with the results using the Approach I, leading to a valid improvement in the ITU signal propagation model, P-1546.

Furthermore, the efficiency of all studied signal propagation models highly depends on the knowledge of the propagation path; therefore, higher resolution digital maps that are regularly updated are essential to guarantee reliable results.

In terms of antenna patterns, this research was conducted in broadcasting frequency band, and all transmitters were omnidirectional. Further studies for other technologies are always recommended; however, accurate antenna pattern of all transmitters, and phase information are required to avoid over/underestimating received fields.

Finally, signals that might be leaking across the borders from transmitters in neighboring countries are seen as outliers as no data is available for these registered antennas. Therefore, dataset exchange for registered antennas with neighboring countries, at least for a specified distance across the borders, would be beneficial in considering these transmitters in the calculations and avoid misidentifying them.

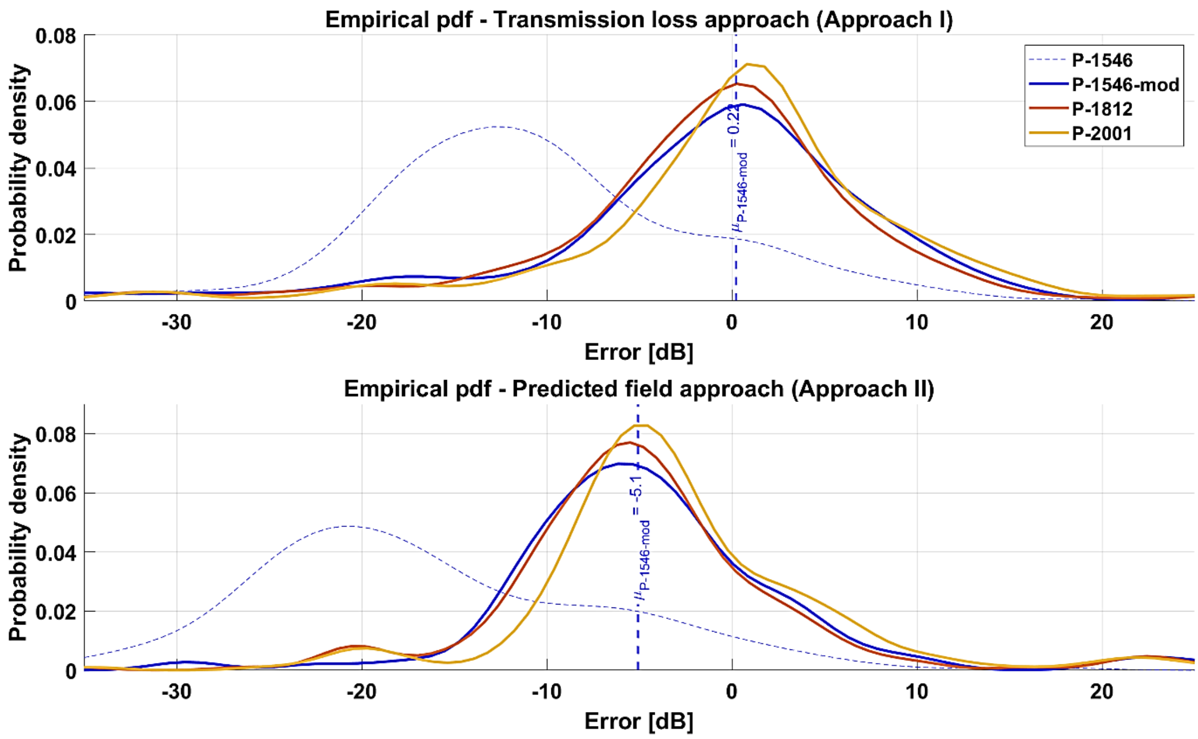


*Figure 13 - Probability density function of error using different approaches.*

# References


[1] ITU, “Recommendation ITU-R P.341-7*, ** - The concept of transmission loss for radio links,” 2019.

[2] C. Huygens, *Treatise on light: In which are explained the causes of that which occurs in reflexion, & in refraction*. 1690.

[3] ITU, “Recommendation ITU-R P.530-18 Propagation data and prediction methods required for the design of terrestrial line-of-sight systems P Series Radiowave propagation,” 2022.

[4] ITU, “Recommendation ITU-R P.617-5( - Propagation prediction techniques and data required for the design of trans-horizon radio-relay systems,” 2019.

[5] ITU, “Recommendation ITU-R P.531-15 (08/2023) - Ionospheric propagation data and prediction methods required for the design of satellite networks and systems,” 2023.

[6] ITU, “Recommendation ITU-R P.1622-1 - Prediction methods required for the design of Earth-space systems operating between 20 THz and 375 THz,” 2022.

[7] ITU, “Recommendation ITU-R P.1546-6( - Method for point-to-area predictions for terrestrial services in the frequency range 30 MHz to 4 000 MHz,” 2019.

[8] ITU, “Recommendation ITU-R P.1812 A path-specific propagation prediction method for point-to-area terrestrial services in the frequency range 30 MHz to 6 GHz,” 2023.

[9] ITU, “Recommendation ITU-R P.2001-5 (08/2023) - A general purpose wide-range terrestrial propagation model in the frequency range 30 MHz to 50 GHz,” 2023.

[10] ITU, “Spectrum Monitoring - Handbook,” 2011.

[11] ITU, “Software.” Accessed: Nov. 13, 2024. [Online]. Available: https://www.itu.int/en/itu-r/study-groups/rsg3/pages/iono-tropo-spheric.aspx

[12] *2011 IEEE-APS Topical Conference on Antennas and Propagation in Wireless Communications : IEEE APWC ’11, 1st edition : proceedings : September 12-16, 2011, Torino, Italy*. IEEE, 2011.

[13] X. Hai, R. Zhang, L. K. Lin, and X. Yu, “Measurement and Analysis of Point-to-Area Propagation at VHF Band,” in *13th International Symposium on Antennas, Propagation and EM Theory, ISAPE 2021 - Proceedings*, Institute of Electrical and Electronics Engineers Inc., 2021. doi: 10.1109/ISAPE54070.2021.9753263.

[14] F. Macedo da Costa, L. Alberto Rabanal Ramirez, and M. Henrique Costa Dias, “Analysis of ITU-R VHF/UHF propagation prediction methods performance on irregular terrains covered by forest,” 2018, doi: 10.1049/iet-map.2017.0992.

[15] “TUNING OF THE PROPAGATION MODEL ITU-R P.1546 RECOMMENDATION.”

[16] C.-H. Lee, Y.-W. Kwak, S.-C. Kim, and S.-H. Bae, “Evaluation of ITU-R Recommendation P.1546 and Consideration for New Correction Factor”.

[17] E. E. Erik¨ostlin, H. Suzuki, and H.-J. Zepernick, “Evaluation of a New Effective Antenna Height Definition in”.

[18] “Comparison of field-strength measurements with simulation results for analog FM broadcasting.”

[19] “Optimal Propagation Model for DVB-T2 System in Urban Area.”

[20] B. Da Silva Duarte and M. H. Costa Dias, “Critical analysis of ITU-R P.1812 and Egli propagation models for LoRaWAN Networks,” *2022 Symposium on Internet of Things, SIoT 2022*, 2022, doi: 10.1109/SIOT56383.2022.10070230.

[21] D. R. C. Aguiar, H. T. P. Silva, H. S. Silva, and U. S. Dias, “Enhancing Signal Prediction Across Brazil: A Clutter Mapping Module for the ITU-R P.1812,” 2024.

[22] ITU, “Attenuation by atmospheric gases P Series Radiowave propagation.”

[23] ITU, “Recommendation ITU-R P.838-3 - Specific attenuation model for rain for use in prediction methods,” 1992.

[24] I. S. Lee, J. H. Noh, and S. J. Oh, “A Survey and analysis on a troposcatter propagation model based on ITU-R recommendations,” *ICT Express*, vol. 9, no. 3, pp. 507–516, Jun. 2023, doi: 10.1016/J.ICTE.2022.09.009.

[25] M. Kvicera *et al.*, “Short-term terrain diffraction measurements from L- to Q-band: Results and analysis,” *IEEE Trans Antennas Propag*, vol. 62, no. 7, pp. 3693–3701, 2014, doi: 10.1109/TAP.2014.2316283.

[26] ITU, “Effects of building materials and structures on radiowave propagation above about 100 MHz P Series Radiowave propagation,” 2015.

[27] C. A. Balanis, *ANTENNA THEORY ANALYSIS AND DESIGN THIRD EDITION*.

[28] A. F. . Molisch, *Wireless communications*. Wiley : IEEE, 2011.

[29] “Means and Medians: When To Use Which - Research Collective.”

[30] RDI, “Antenna Ragister.” Accessed: Nov. 18, 2024. [Online]. Available: https://antenneregister.nl/Html5Viewer/Index.html?viewer=Antenneregister%5Fextern

[31] ITU, “Recommendation ITU-R P.526-15 - Propagation by diffraction”.

[32] ITU, “Recommendation ITU-R P.310-10 - Definitions of terms relating to propagation in non-ionized media,” 2019.

# Appendix A

## “Smooth-Earth” model and effective antenna heights.

The smooth-earth model is a model to calculate the effective antenna heights of both terminals which is later used for the diffraction model and the assessment of the roughness of the propagation path required by the ducting-layer reflection model.

As explained in 2.2, the propagation mode P-1812 splits the total propagation path into multiple equal sections identifying the begin of a new section with a point called profile point.

This model replaces the tertian between the transmitter and the receiver with a smooth surface and define the smooth-earth height at the transmitter, $h_{st}$, and the receiver, $h_{sr}$, according to the parameters, $v_1$ & $v_2$, which are normalized parameters that takes into account the terrain height and the distance to transmitter of each profile point.

$$v_1 = \sum_{i=1}^{n} (d_i - d_{i-1})(h_i + h_{i+1})$$

$$v_2 = \sum_{i=1}^{n} (d_i - d_{i-1})[h_i(2d_i + d_{i-1}) + h_{i-1}(d_i + 2d_{i-1})]$$

$i$ : number of profile point

$d_i$ : distance between the $i^{th}$ profile point and the transmitter.

$h_i$ : terrain height at the $i^{th}$ profile point.

These parameters define the smooth-earth height at Tx & Rx as:

$$h_{st} = \frac{2v_1 d - v_2}{d^2} \qquad h_{sr} = \frac{v_2 - v_1 d}{d^2} \qquad (4)$$

The modification proposed in trail “b” of section “Terrain height effect” suggest that scaling these parameters, $v_1$&$v_2$, according to the variation of the terrain height along the propagation path, named $h_{tot}$, can reduce the risk of over simplifying the propagation path especially for lower number of profile points and in areas where the terrain varies a lot along the propagation path.

The modified parameters are then given by:

$$v_{1\,new} = v_1 * \sigma_{h_{tot}} \qquad v_{2\,new} = v_2 * \sigma_{h_{tot}}$$

$\sigma_{h_{tot}}$ : standard deviation of the terrain height along the total propagation path

The new smooth-earth heights at Tx & Rx are then calculated by equation (4) using the new definition of the normalized parameters.

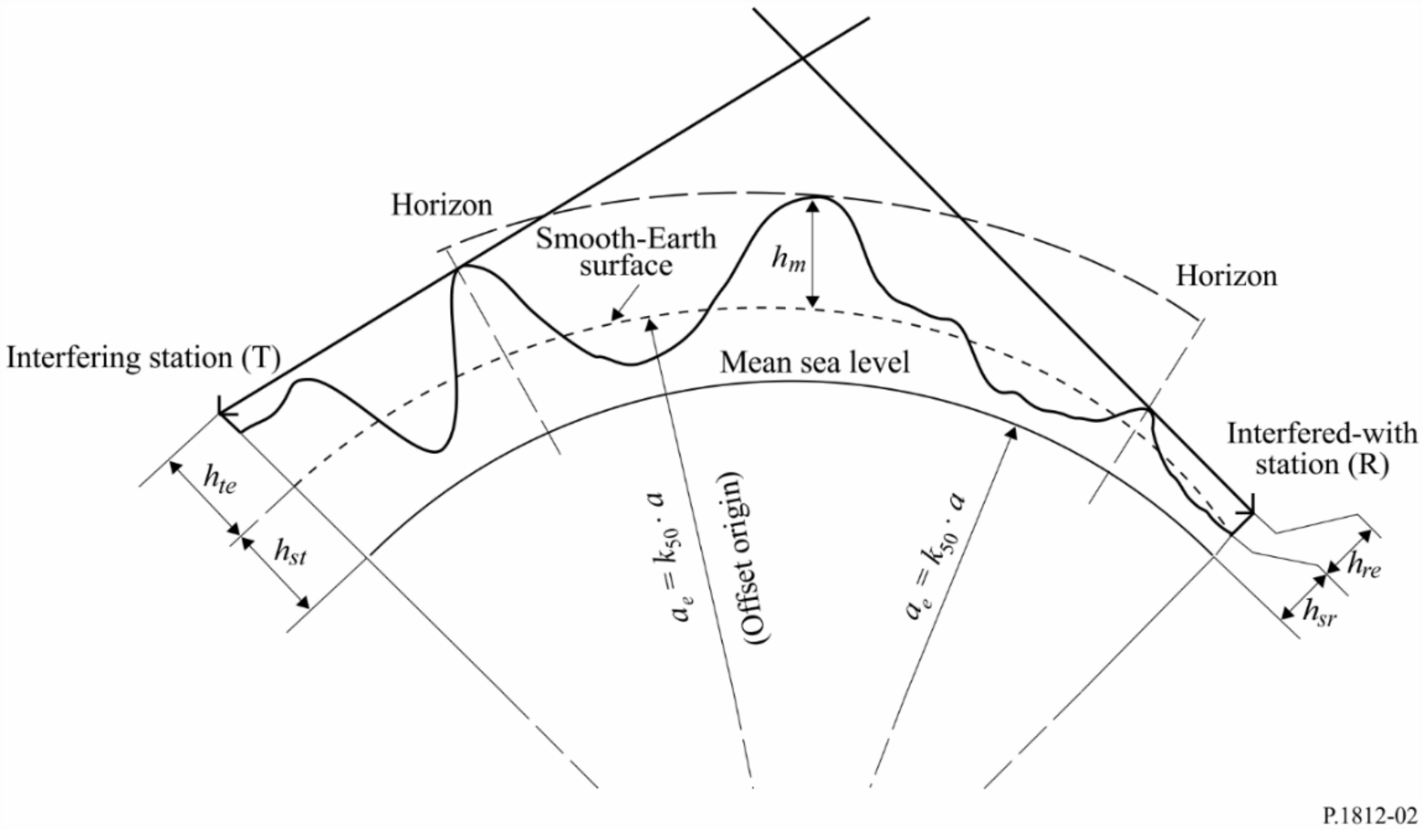


*Figure 14 - Illustration of "Smooth-Earth" model [8].*

# Appendix B

*Table B. 1 - Median error per location (dB).*

| | P-1546 | P-1546-mod | P-1812 | P-2001 | Free Space |
|---|---|---|---|---|---|
| **AMSTELVEEN** | -8.6 | -1.9 | -0.5 | 1.0 | 10.6 |
| **AXEL** | -10.4 | 0.2 | -0.9 | -0.8 | 10.5 |
| **BREDA** | -13.0 | -0.3 | 0.1 | 0.3 | 2.5 |
| **EINDHOVEN** | -14.1 | 1.0 | 0.3 | 2.2 | 7.4 |
| **GRONINGEN** | -4.8 | -0.1 | -0.5 | -0.1 | 11.0 |
| **HEERHUGOWARD** | -7.9 | -1.7 | 1.5 | 2.1 | 12.5 |
| **HENGELO** | -13.0 | 1.4 | 1.7 | 2.2 | 11.0 |
| **Hoek van Holland** | -13.1 | -4.5 | -1.2 | 0.5 | 13.3 |
| **HOOGEVEEN** | -15.5 | -5.5 | -5.5 | -2.3 | 13.9 |
| **LEEUWARDEN** | -11.2 | -2.1 | -2.1 | -1.1 | 20.0 |
| **NIJMEGEN** | -13.0 | 0.6 | -1.9 | -1.2 | 6.8 |
| **SCHIEDAM** | -15.4 | -0.6 | -4.2 | 0.6 | 8.6 |
| **SITTARD** | 8.4 | 8.5 | 8.4 | 8.4 | 9.6 |
| **'t HARDE** | -8.6 | 11.2 | 10.4 | 13.6 | 18.0 |
| **WIJDEMEREN** | -13.5 | 1.5 | 1.1 | 1.9 | 10.9 |

# Appendix C

*Table C. 1 - MAPE per location (dB).*

| | P-1546 | P-1546-mod | P-1812 | P-2001 | Free space |
|---|---|---|---|---|---|
| **AMSTELVEEN** | 17.5 | 5.5 | 4.3 | 4.0 | 8.8 |
| **GRONINGEN** | 26.2 | 6.4 | 10.9 | 7.5 | 25.3 |
| **HENGELO** | 21.9 | 9.5 | 15.7 | 12.9 | 22.9 |
| **HOOGEVEEN** | 26.3 | 11.6 | 10.4 | 11.2 | 22.5 |
| **SCHIEDAM** | 25.2 | 11.9 | 6.1 | 6.2 | 48.3 |
| **NIJMEGEN** | 19.9 | 13.5 | 6.0 | 6.7 | 42.7 |
| **Hoek van Holland** | 18.7 | 15.3 | 8.4 | 10.7 | 30.8 |
| **Breda** | 27.0 | 15.6 | 16.9 | 15.7 | 20.2 |
| **‘t Harde** | 23.9 | 15.9 | 14.9 | 14.3 | 16.0 |
| **Sittard** | 27.3 | 15.9 | 11.2 | 12.8 | 31.1 |
| **Leeuwarden** | 28.0 | 21.4 | 20.6 | 21.3 | 26.9 |
| **Axel** | 35.8 | 23.0 | 18.9 | 12.8 | 35.8 |
| **Eindhoven** | 29.9 | 25.3 | 25.5 | 26.3 | 19.4 |
| **Heerhugoward** | 29.3 | 26.3 | 24.0 | 24.9 | 20.6 |
| **Wijdemeren** | 17.6 | 35.4 | 32.5 | 39.2 | 47.0 |